MAGNETOELASTIC PROPERTIES OF RARE-EARTH ELEMENTS AND COMPOUNDS

SEMIANNUAL REPORT

5 November 1971 - 4 May 1972

MATERIALS SCIENCE LABORATORY

RICE UNIVERSITY

HOUSTON, TEXAS

Paul L. Donoho

Franz R. Brotzen

Kamel Salama

L. V. Benningfield, Jr.

Work Performed Under Contract No. DAAH01-72-C-0285

Effective Date: 5 November 1971

Expiration Date: 4 November 1972

Contract Amount: $119,218.00

Program Code: A3168Z

Monitored by U. S. Army Missile Command

R. L. Norman, Project Manager

Sponsored by:

Advanced Research Projects Agency

ARPA Order Nr. 1685

Unclassified
Security Classification

DOCUMENT CONTROL DATA - R & D
(Security classification of title, body of abstract and indexing annotation must be entered when the overall report is classified)

1. ORIGINATING ACTIVITY (Corporate author)
Rice University
Materials Science Laboratory
Houston, Texas 77001

2a. REPORT SECURITY CLASSIFICATION
Unclassified

2b. GROUP

3. REPORT TITLE
Magnetoelastic Properties of Rare-Earth Elements and Compounds

4. DESCRIPTIVE NOTES (Type of report and inclusive dates)
Semiannual Technical Report 5 November 1971 - 4 May 1972

5. AUTHOR(S) (First name, middle initial, last name)
Paul L. Donoho, Franz R. Brotzen, Kamel Salama, and L. V. Benningfield, Jr.

6. REPORT DATE
4 June 1972

7a. TOTAL NO. OF PAGES
114

7b. NO. OF REFS
43

8a. CONTRACT OR GRANT NO.
DAAH01-72-C-0285

b. PROJECT NO.

c.

d.

9a. ORIGINATOR'S REPORT NUMBER(S)

9b. OTHER REPORT NO(S) (Any other numbers that may be assigned this report)

10. DISTRIBUTION STATEMENT
Distribution of this document is unlimited

11. SUPPLEMENTARY NOTES

12. SPONSORING MILITARY ACTIVITY
Advanced Research Projects Agency,
Arlington, Virginia 22209

13. ABSTRACT

This report describes the technical accomplishments attained during the third six-month period of a research program on the magnetic and magnetoelastic properties of rare-earth elements, alloys, and compounds. The primary goal of this program is the development of applications which utilize the extremely large magnetostriction exhibited by most rare-earth materials. The research carried out during the period covered by this report has been concentrated in three major areas;

1. Studies on elastic-wave propagation in terbium at frequencies in the megahertz range have shown the existence of very strong field-induced acoustic birefringence in single-crystal specimens. Such an effect leads to the possibility of the construction of the acoustic analog of such optical devices as the quarter-wave plate or such microwave devices as the isolator and circulator.

2. Magnetostrictive ultrasonic transducers in the form of thin polycrystalline films have been constructed using several pure rare-earth elements and a terbium-iron compound. Such transducers have been studied at frequencies from 700 MHz to 1.4 GHz, at temperatures from 4.2K to room temperature. In all cases, the magnetostrictively generated elastic waves, whose intensities were magnetic-field dependent, were quite strongly generated, with generation efficiencies as large as two orders of magnitude

(cont'd - p.2)

DD FORM 1 NOV 1473

Unclassified
Security Classification

Abstract, (cont'd)

greater than that for piezoelectric generation in quartz. Preliminary results indicate that still higher efficiency can be attained.

3. A semiclassical theory of magnetoelastic interactions in rare-earth materials, which is based on an equation-of-motion approach to the dynamical behavior of magnetic materials, has yielded results which are applicable to both the two preceding areas of research and which, in particular, should make possible the design of more efficient microwave ultrasonic transducers.

In addition to the three major areas of research listed above, work has also been carried out on the preparation of rare-earth-iron-group intermetallic compounds, particularly the rare-earth iron compounds, such as $TbFe_2$, which exhibit large room-temperature magnetostriction in polycrystalline specimens. Finally, work is underway on a project to measure magnetostriction in rare-earth materials by means of holographic interferometry. Preliminary results indicate that this method will prove particularly valuable for measurements on small, irregularly shaped samples and in cases where shear magnetostrictive strain is observed.

14 KEY WORDS	LINK A		LINK B		LINK C	
	ROLE	WT	ROLE	WT	ROLE	WT
Rare Earths						
Elements and Compounds						
Magnetostriction						
Magnetoelastic Properties						
Ultrasonic Transducers						
Ultrasonic Propagation						

MAGNETOELASTIC PROPERTIES OF RARE-EARTH ELEMENTS AND COMPOUNDS

SEMIANNUAL REPORT

5 November 1971 - 4 May 1972

MATERIALS SCIENCE LABORATORY

RICE UNIVERSITY

HOUSTON, TEXAS

Paul L. Donoho

Franz R. Brotzen

Kamel Salama

L. V. Benningfield, Jr.

Work Performed Under Contract No. DAAH01-72-C-0285

Effective Date: 5 November 1971

Expiration Date: 4 November 1972

Contract Amount: $119,218.00

Program Code: A3168Z

Monitored by U. S. Army Missile Command

R. L. Norman, Project Manager

Sponsored by:

Advanced Research Projects Agency

ARPA Order Nr. 1685

d

TABLE OF CONTENTS

LIST OF FIGURES

Page No.

Page No.

Page No.

LIST OF TABLES

ABSTRACT

This report describes the technical accomplishments attained during the third six-month period of a research program on the magnetic and magnetoelastic properties of rare-earth elements, alloys, and compounds. The primary goal of this program is the development of applications which utilize the extremely large magnetostriction exhibited by most rare-earth materials. The research carried out during the period covered by this report has been concentrated in three major areas:

1. Studies on elastic-wave propagation in terbium at frequencies in the megahertz range have shown the existence of very strong field-induced acoustic birefringence in single-crystal specimens. Such an effect leads to the possibility of the construction of the acoustic analog of such optical devices as the quarter-wave plate or such microwave devices as the isolator and circulator.

2. Magnetostrictive ultrasonic transducers in the form of thin polycrystalline films have been constructed using several pure rare-earth elements and a terbium-iron compound. Such transducers have been studied at frequencies from 700 MHz to 1.4 GHz, at temperatures from 4.2K to room temperature. In all cases, the magnetostrictively generated elastic waves, whose intensities were

magnetic-field dependent, were quite strongly generated, with generation efficiencies as large as two orders of magnitude greater than that for piezoelectric generation in quartz. Preliminary results indicate that still higher efficiency can be attained.

3. A semiclassical theory of magnetoelastic interactions in rare-earth materials, which is based on an equation-of-motion approach to the dynamical behavior of magnetic materials, has yielded results which are applicable to both the two preceding areas of research and which, in particular, should make possible the design of more efficient microwave ultrasonic transducers.

In addition to the three major areas of research listed above, work has also been carried out on the preparation of rare-earth-iron-group intermetallic compounds, particularly the rare-earth iron compounds, such as $TbFe_2$, which exhibit large room-temperature magnetostriction in polycrystalline specimens. Finally, work is underway on a project to measure magnetostriction in rare-earth materials by means of holographic interferometry. Preliminary results indicate that this method will prove particularly valuable for measurements on small, irregularly shaped samples and in cases where shear magnetostrictive strain is observed.

I. INTRODUCTION

This report describes the technical accomplishments attained in the course of a research program on the magnetic and magnetoelastic properties of the rare-earth elements and on alloys and compounds containing the rare earths. This program is sponsored by the Advanced Research Projects Agency of the Department of Defense (ARPA Order No. 1685), and it is administered by the U. S. Army Missile Command under Contract No. DAAH01-72-C-0285. This report covers work performed during the period 5 November 1971 through 4 May 1972. This period represents the third six-month period of ARPA sponsorship of this program, which was supported for the year ending 1 November 1971 under Contract No. DAAH01-71-C-0259[1].

The primary goal of this research program is the development of new technical applications of rare-earth materials based upon the extremely large magnetoelastic coupling exhibited by most rare-earth elements, alloys, and compounds. In particular, the major effort is directed toward the development of highly efficient ultrasonic transducers capable of operation at frequencies up to the microwave range. Such transducers would produce intense ultrasonic beams which would find numerous applications in the areas of the nondestructive testing of materials, the inves-

tigation of nonlinear elastic properties of solids, high-frequency acoustical holography, and microwave communications and signal-processing systems. In addition to the direct generation of ultrasonic waves by means of magnetostriction, various other applications based upon the strong magnetoelastic coupling in the rare earths are possible. Strongly field-dependent attenuation and velocity dispersion of elastic waves at frequencies as low as 10-20 MHz lead to the possibility of the development of acoustic modulators and variable delay lines. Field-induced acoustic birefringence, which is reported here, leads to the possibility of various nonreciprocal acoustic circuit elements, analogous to microwave isolators and circulators or to optical quarter-wave plates. Although the pure rare earths and many of their alloys with each other exhibit large magnetostriction only in a single-crystal state and at cryogenic temperatures, the recent discovery by Clark and Belson[2] that compounds such as $TbFe_2$ exhibit extremely large magnetostriction at room temperature and higher and in polycrystalline form should make possible the development of applications of the types mentioned above without the restriction of operation only at cryogenic temperatures.

The research described in this report may be divided into the following major areas, of which the first three represent approximately 90 per cent of the total effort, while the remaining two

areas represent new work which is just beginning to yield results at this time:

1. Elastic-Wave Propagation in the Rare Earths

A major effort has been placed since the inception of this peoject upon attempts to determine the elastic properties of the pure rare earths and the other rare-earth materials of interest and to determine the ways in which the magnetoelastic coupling affects the propagation of elastic waves in these materials. Such work was summarized to a large extent in the annual report for the previous year's work[1], and the results obtained for the elastic constants of terbium and holmium are to be published[3,4]. During the period covered by the present report, the major effort has been directed toward the investigation of shear-wave propagation along the hexagonal axis in single-crystal terbium. An investigation of the elastic properties of polycrystalline terbium was also carried out, and an investigation of elastic-wave propagation in single-crystal dysprosium was begun.

The most interesting results are those arising from the study of elastic-wave propagation along the hexagonal axis in single-crystal terbium. In terbium below the magnetic ordering temperature, T_N = 229K, the magnetization is constrained by a very large uniaxial anisotropy to lie in the basal plane of the

hcp crystal structure. For shear elastic waves propagating along the hexagonal axis there is a magnetoacoustic birefringence resulting from the shear magnetoelastic coupling, such that the wave velocity for polarization along the magnetization is different from that for waves polarized perpendicular to the magnetization. If a wave is initially generated in a terbium sample with its polarization at an angle of 45° to the direction of the magnetization, then its polarization changes as it propagates along the hexagonal axis. As the two components traveling at different velocities get slightly out of phase, the polarization can be described as elliptical, in analogy with the optical case. When the waves are exactly one-quarter wavelength out of phase, the polarization is circular, leading to the possibility of the development of a simple acoustic quarter-wave plate. As the wave travels further along the hexagonal axis, its polarization again becomes linear, but it is now directed perpendicular to the original polarization direction. If the wave now encounters the original transducer, as a result of being reflected from a free surface of the rare earth, for example, it will not induce the usual ultrasonic echo in the transducer.

The application of a magnetic field in the basal plane of the sample will cause the magnetization to vary, thus changing the difference in wave velocities. Thus, in the usual ultrasonic

echo arrangement, if the shear-wave transducer is polarized at 45° to the field direction, variation of the magnetic field will lead to a field-dependent oscillation of the amplitude of the detected echoes. Such oscillations have been observed, and measurement of their period leads to a determination of the shear magnetostrictive coupling, as reported in the following section of this report. Since it appears that the shear magnetoelastic coupling is largely responsible for the magnetostrictive ultrasonic generation which is also described in this report, this ability to measure the strength of this coupling by means of the magnetoacoustic birefringence is extremely valuable. The measurement of the shear coupling can, in fact, be carried out for terbium in the paramagnetic phase[5] by means of static magnetostriction measurements, but the present method is more sensitive and, with further analysis, it should also be more accurate. The complete description of the work performed on birefringence and its significance is given in Section II.

2. Magnetostrictive Elastic-Wave Generation in Rare Earths and Rare-Earth Compounds.

The original motivation for this research was the possible development of high-efficiency ultrasonic transducers based on the extremely large magnetostriction of many rare-earth materials.

Preliminary work[6] indicated that polycrystalline thin films of several pure rare earths could, indeed, be used successfully as transducers at frequencies as high as 10 GHz, although the difficulty of producing films of high purity on quartz and sapphire substrates led to a complicated vacuum-deposition process, with films of doubtful purity. As a result, the intensity of ultrasonic generation in the preliminary work mentioned above was quite variable, and it never reached the level which was expected from consideration of the large magnetostriction of the bulk pure rare earths.

The present report describes results obtained with films of several rare-earth materials at frequencies from 690 MHz to 1.5 GHz. The efficiency of ultrasonic generation in the present work has been improved over the previous work[6] such that magnetostrictive ultrasonic generation in films of the pure rare earths has now been increased by several orders of magnitude over that reported earlier. Furthermore, the compound $TbFe_2$, recently shown by Clark and Belson[2] to possess very large magnetostriction at room temperature, has been investigated as an ultrasonic transducer over the same frequency range, and it has been found to be fairly efficient at temperatures as high as 350K, somewhat above room temperature.

Although it is expected that single-crystal transducers will ultimately exhibit much higher ultrasonic-generation efficiency

than do polycrystalline films of rare-earth materials, the problems associated with the bonding of such highly magnetostrictive materials to a substrate in which the ultrasonic waves can be observed at high frequencies have proven to be very difficult. Although ultrasonic generation using single-crystal transducers of both terbium and gadolinium has been observed[1], the results are still rather limited, and their reproducibility is poor.

A complete description of the work on magnetostrictive elastic-wave generation in rare-earth materials is given in Section III of this report.

3. Theory of Dynamic Magnetoelastic Properties of the Rare Earths

As discussed in the preceding annual report on this project[1], theoretical attempts to explain dynamic magnetoelastic effects such as ultrasonic generation, elastic-wave velocity dispersion and attenuation, and magnetic resonance, have in the past largely utilized methods which are not particularly appropriate to the rare earths. The rare earths ions in a rare-earth material have highly localized magnetic moments which experience very large crystal-field anisotropy, in contrast to most iron-group magnetic ions. The rare earths are also characterized by very large values of the total angular momentum, in contrast to iron-group ions, for which the orbital angular momentum is usually quenched by crystal-

field effects. An effort has been made, therefore, to develop a theoretical approach to the problems of interest in this research project which takes account of the magnetic and magnetoelastic properties characteristic of rare-earth materials.

The principal feature of the theoretical treatment to be presented in this report is the development of dynamical equations of motion for the elastic-wave variables, treated classically, and for the complete set of tensor angular-momentum operators required to describe completely a quantum-mechanical system of arbitrary angular momentum. These coupled equations of motion, in which the magnetoelastic interaction couples the dynamical lattice variables to the dynamical angular-momentum variables, can be applied to the solution of a variety of problems related to the experimental work being pursued under this research program. In particular, the magnetoacoustic birefringence discussed above and in Section II is readily explained in terms of this new theory. Problems involving velocity dispersion and elastic-wave attenuation can also be treated easily by means of this theory. The question of ultrasonic generation through magnetoelastic coupling is also readily treated. For the systems of interest, however, the complete set of equations of motion necessary for a full treatment of any sort of magnetoelastic problem lead to a formidable problem in numerical analysis. Consequently, only a few specific problems have been

worked out using the theory. The results obtained to the present are presented in Section IV of this report.

4. Preparation of Rare-Earth Iron Intermetallic Compounds

In an effort to prepare specimens of the very interesting compounds RFe_2, where R is any rare earth, which have been shown by Clark and Belson[2] to possess very large magnetostriction at room temperature in polycrystalline specimens, apparatus has been constructed for the purpose of making a series of rare-earth-iron compounds with this or similar composition. Preliminary specimens have been prepared, and they are being analyzed at present. The $TbFe_2$ compounds utilized in the research on ultrasonic generation discussed above and in Section III were obtained commercially. This work is described in Section V of this report.

5. Measurement of Magnetostriction by Holographic Interferometry

The most widely employed method for the measurement of static magnetostriction has been in recent years the direct measurement of magnetostrictive strain by means of strain gauges attached to the specimens of interest. The strain-gauge technique requires, however, the use of relatively large, regularly shaped, specimens of the material to be studied. Furthermore, the strain-gauge can yield information concerning shear strains only through a difficult

interpretation of data obtained from strain gauges attached to the sample in such a manner as to measure longitudinal strain along certain special directions. In addition, the strain-gauge method cannot detect the presence of nonuniform magnetostrictive strain, which may be present in some types of rare-earth materials.

An effort has been started, therefore, to measure magnetostrictive strains of all types by means of holographic interferometry. In this method, an interference pattern is formed as a result of coherent light striking a magnetostrictively deformed specimen and a reconstructed holographic image of the unstrained specimen. A straightforward analysis of the interference pattern then permits a complete determination of the strain in the specimen, even in the case of specimens too small or too irregular for the attachment of strain gauges. This method has been applied to such materials as $TbFe_2$ in polycrystalline form, yielding results in agreement with those obtained with strain-gauge techniques. Cryogenic apparatus is planned to permit the method to be applied to the pure rare earths and to alloys which require low temperatures. This work is described in more detail in Section V of this report.

II. ELASTIC WAVE PROPAGATION IN RARE EARTHS

The investigation of magnetoelastic effects on the propagation of elastic waves in the rare earths at frequencies in the range 10-50 MHz has yielded useful information concerning the magnetoelastic coupling, and such investigations have often led to new insight into the nature of magnetoelastic phenomena in these materials. In this report, two areas of investigation are described: The observation of shear-wave propagation along the hexagonal axis in single-crystal terbium has led to a measurement of shear magnetoelastic coupling in ferromagnetic and helimagnetic terbium, a result which can be obtained by no other currently available technique; measurements on the magnetic-field dependence of ultrasonic attenuation in polycrystalline terbium have led to results which constitute a useful complement to earlier results obtained with single-crystal terbium. These two investigations are described separately in what follows.

1. Shear Magnetoelastic Coupling in Terbium

The interaction of elastic waves with the magnetic moments of ions in a magnetically ordered solid, often described on the quantum-mechanical level as the spin-wave-phonon interaction, was first discussed by Turov and Irkhim[7], and this problem was subse-

quently treated by Kittel[8] and by Akhiezer et al.[9] Later, the problem was treated in considerable detail by Schlömann[10]. Experimental observations of microwave-frequency ultrasonic generation in thin films of iron-group materials by Seavey[11] and in thin films of rare-earth materials by Maley et al.[6] confirmed many of the theoretical predictions of Schlömann and the earlier authors. Among the theoretical predictions of Schlömann most pertinent to the present work is the phenomenon of magnetoacoustic birefringence. Under a variety of experimental conditions, shear waves propagated along a crystallographic axis for which the two shear modes are normally degenerate in velocity can exhibit the effects associated with optical birefringence. The effects arise from the coupling of the elastic waves to the magnetization of the crystal, and they are expected to be particularly important when the phase velocity of the shear waves is near that of the spin waves. This magnetoacoustic birefringence has been observed in several cases[12-15] in iron-group magnetic materials at very high frequencies. The rare-earth materials, which exhibit much stronger magnetoelastic coupling than do the iron-group elements, provide an ideal opportunity for the observation of magnetoacoustic birefringence at relatively low frequency ($\leq$ 50 MHz), where generation and detection of elastic waves is particularly simple. In fact, the large magnetoelastic coupling found in such pure rare

earths as terbium makes possible the application of the magneto-acoustic birefringence to the development of such devices as acoustic isolators or circulators.

Two principal birefringence effects should be observable in the rare earths at frequencies in the megahertz range:

1. If the magnetization of the specimen is parallel to the propagation vector of the shear elastic waves, a circular birefringence, analogous to that found in optically active materials, is induced, such that the plane of polarization of a linearly polarized shear wave rotates about the propagation axis as the wave travels along this axis. The amount of rotation per unit length of travel along the axis depends, among other things, on the strength of the shear magnetoelastic coupling, which determines the difference in velocity between the two independent circularly polarized waves which can propagate along the axis. This effect is not observed in the normal pulse-echo ultrasonic experiment, since the direction of roation of the plane of polarization is reversed when waves are reflected from a free surface, returning to its original direction when the waves return to the transducer at which they were generated. Furthermore, in the work reported here, which utilized terbium as the material of interest, the difficulty of obtaining a substantial magnetization parallel to the hexagonal axis also prevented the observation of circular birefringence.

2. The second birefringence effect, and the one for which experimental results are reported below, is a linear birefringence which can occur when the magnetization of the material is perpendicular to the axis of propagation of the shear waves. In this case, the velocity for waves polarized parallel to the magnetization is different from that for waves polarized perpendicular to the magnetization. This situation is analogous to normal optical birefringence. Thus, a wave initially polarized parallel to or perpendicular to the magnetization will remain linearly polarized, but a wave whose initial linear polarization makes an angle of 45° with the direction of the magnetization will become generally elliptically polarized as it propagates along the axis. In fact, the wave will first become elliptically polarized, and, then, as the phase difference between the polarization components parallel to and perpendicular to the magnetization reaches 90°, it becomes circularly polarized. When the phase difference reaches 180°, the wave is again linearly polarized, but in a direction normal to the original direction of polarization. It is this aspect of the birefringence which makes it easily detectable in a pulse-echo ultrasonic experiment. Furthermore, terbium, in which the magnetization is constrained to lie in the basal plane, perpendicular to the hexagonal axis, and in which the magnetoelastic coupling is extremely large, is an ideal material for the observation of this linear magnetoacoustic birefringence at relatively low frequency.

In this report, the first observation of linear birefringence in a rare-earth crystal is reported. Previous ultrasonic studies of elastic-wave velocity in the rare earths have only revealed such effects as the anomalous attenuation and velocity near magnetic phase transitions[16,17]. In what follows, the treatment of Schlömann[10], in which magnetoacoustic birefringence was predicted is outlined. The experimental results of the work reported here are then presented and compared with the theoretical treatment. A somewhat different theoretical approach to the same problem is given in Section IV of this report.

In his treatment of spin-wave-elastic-wave interactions, Schlömann develops coupled wave equations for the spin waves and the elastic waves. In regions where the phase velocities of the two types of wave are appreciably different, the interaction effects are small, and the waves are nearly the same as if there were no magnetoelastic coupling. Where the phase velocities are nearly equal, however, the waves can be described only as coupled magnetoelastic waves, with characteristics different from those of either type of uncoupled wave. For transverse elastic waves propagating along the hexagonal axis of an hcp crystal, dispersion relations for the coupled elastic and spin waves take the following form when the elastic-wave polarization is parallel to the magnetization[16]:

$$(\omega^2-v^2k^2)(\omega^2-\omega_m^2) = \sigma\gamma H_i v^2 k^2 \quad . \tag{1}$$

When the polarization is perpendicular to the magnetization, the following uncoupled dispersion relationship is obtained:

$$(\omega^2-v^2k^2)(\omega^2-\omega_m^2) = 0 \tag{2}$$

In Equations (1) and (2), ω and v are, respectively, the angular frequency and phase velocity of the elastic wave, ω_m and k are the angular frequency and wave vector of the spin wave, γ is the gyromagnetic ratio of the magnetic ions, σ is the magnetoelastic interaction strength, and H_i is the internal magnetic field strength. For the case in which the magnetization is parallel to the b-axis, the easy axis of magnetization in terbium, the spin angular frequency and the internal field are given by[18]

$$\omega_m^2 = \gamma^2 (H-NM-36\frac{K_6^6}{M^6})\ (H-NM+4\pi M + 2\frac{K_2}{M} - 6\frac{K_6^2}{M}) \tag{3}$$

$$H_i = (H-NM-36\frac{K_6^6}{M}) \quad , \tag{4}$$

where NM is the demagnetizing field, K_6^6 is the basal-plane sixfold anisotropy, and K_2 is the uniaxial anisotropy free energy. In the limit $\omega \ll \omega_m$, the relative phase difference between waves polarized parallel to and perpendicular to the magnetization, expressed in radians per unit length of travel along the hexagonal axis, is found to be the following:

$$\emptyset/\ell = (\omega\sigma/2\gamma v)\,[H-C_2]^{-1} = C_1/(H-C_2) \qquad (5)$$

In this expression, C_2 is a constant which depends upon the demagnetizing field and the effective anisotropy fields. In terms of the shear magnetostriction, the interaction strength is given by $\sigma = \gamma b^2/\rho M v^2$, where ρ is the density of the crystal and b is the shear magnetoelastic constant. Experimentally, the values of the phase shift, $\emptyset$, for which the elastic-wave polarization is perpendicular to the original direction (which is determined by the transducer orientation), can be determined as the applied magnetic field is varied. From the observed field values at which the detected elastic-wave amplitude reaches a minimum, the magneto-elastic coupling, b can be determined.

The terbium single crystal used in this work, and also used in previously reported work[1], was fabricated by Metals Research Ltd., Cambridge, U.K., in the form of a cylinder 6 mm in diameter and 25 mm in length. A specimen 6 mm in length was prepared using a spark-machining technique with two faces normal to the hexagonal c-axis within one degree. The specimen was then electropolished to remove cold-worked layers. An AC-cut quartz transducer of fundamental frequency 10 MHz and diameter 3 mm was acoustically bonded to one of the parallel faces of the terbium specimen with Dow Corning V-9 silicone material. The transducer was oriented

such that the polarization vector of piezoelectrically generated transverse elastic waves was parallel to the b-axis of the terbium crystal. Thus, the transducer was capable of detecting only echoes with this same polarization direction, or at least a polarization component along the b-axis.

A conventional commercial ultrasonic pulse-echo transmitter-receiver system (Matec, Inc. Model 760 RF Plug-In in Model 6000 Mainframe) was used for both the generation and detection of 30 MHz shear elastic waves. The amplitude of any desired ultrasonic echo could be monitored by means of a boxcar integrator (Matec, Inc. Model 1235A) whose output was applied to the y-axis of an x-y recorder. A magnetic field as high as 18.3 kOe could be applied to the sample in a direction lying in the basal plane at an angle of 45° to the b-axis along which the transducer polarization was directed. A Hall-effect gaussmeter was used to monitor the magnetic-field strength, and its output was applied to the x-axis of the x- recorder. Thus, the amplitude of any desired echo could be recorded as a function of the applied magnetic-field strength.

The specimen was maintained at any desired temperature by means of a standard continuous-flow cryostat in connection with a feedback control system which utilized a copper-constantan thermocouple for both the measurement and control of specimen temperature. With this system, the temperature could be controlled to ± 0.1C at

any desired value below room temperature. The measurement of echo amplitude was always made as a function of increasing magnetic field at constant temperature, and the temperature was always decreased from one measurement to the next.

In order to determine the crystallographic orientation of the single-crystal terbium specimen after its insertion into the cryogenic system, the angular dependence of the elastic-wave velocity was measured at high magnetic-field strength. A typical example of the results obtained at a temperature of 240K and a magnetic field of 10 kOe is shown in Fig. 1. The apparatus and the method for obtaining these data are described elsewhere[4]. It can be seen from Fig. 1 that the velocity is a maximum when the magnetic field is applied perpendicular to the direction of polarization. When the field is parallel to the polarization, the velocity is minimized. These results are similar to those obtained by Moran and Lüthi[16]. The primary interest in this angular dependence of the elastic-wave velocity in the work reported here is, however, the exact determination of the b-axis along which the polarization is directed after the specimen is placed into the cryostat.

In Fig. 2 a set of curves is shown representing the change in the ultrasonic echo amplitude as a function of the applied magnetic field. These curves were obtained at a temperature of 230K using

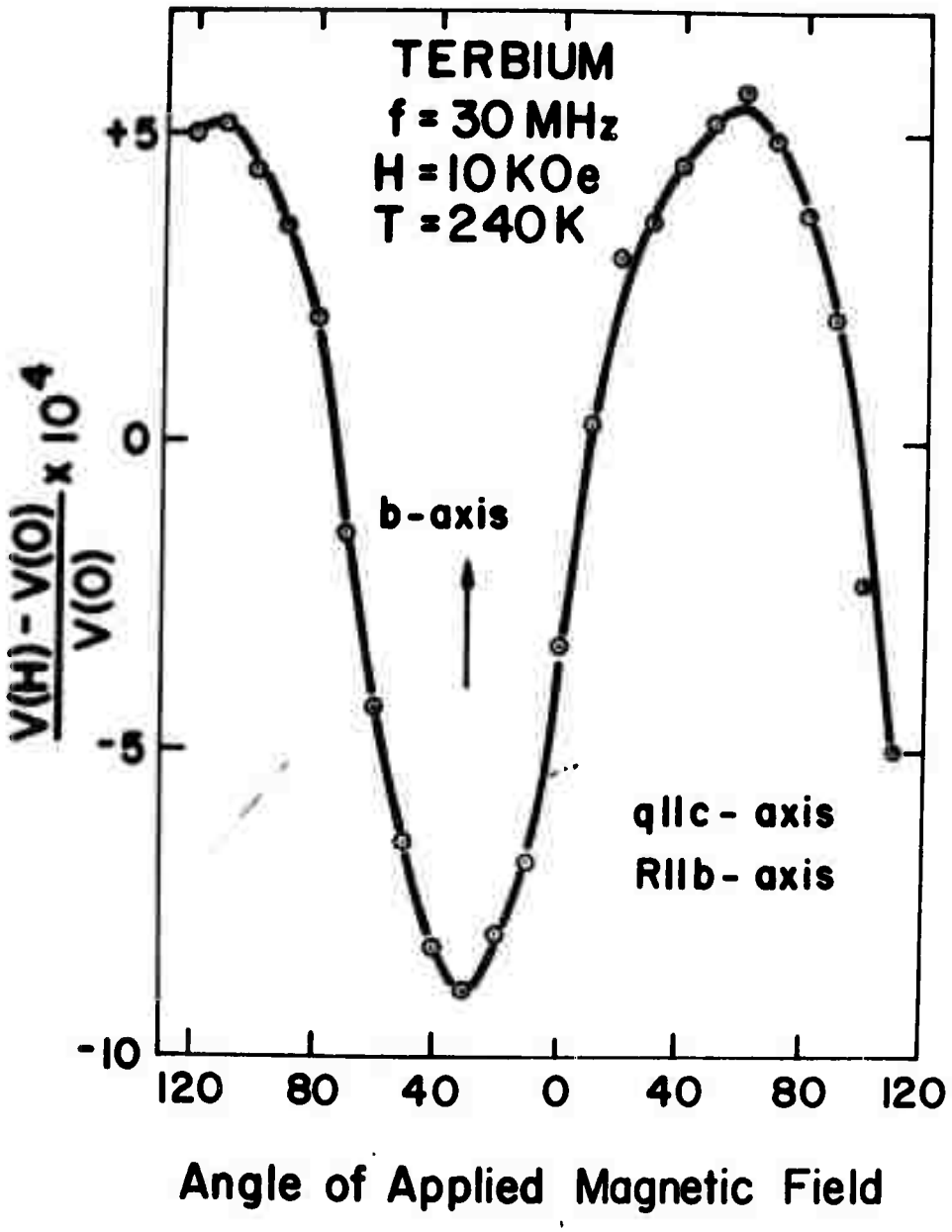

Fig. 1 Magnetic-field angular dependence of the relative change in the velocity of transverse elastic waves propagating along the c-axis of a terbium single crystal at a temperature of 240 K. The applied field is 10 kOe, the polarization is parallel to the b-axis.

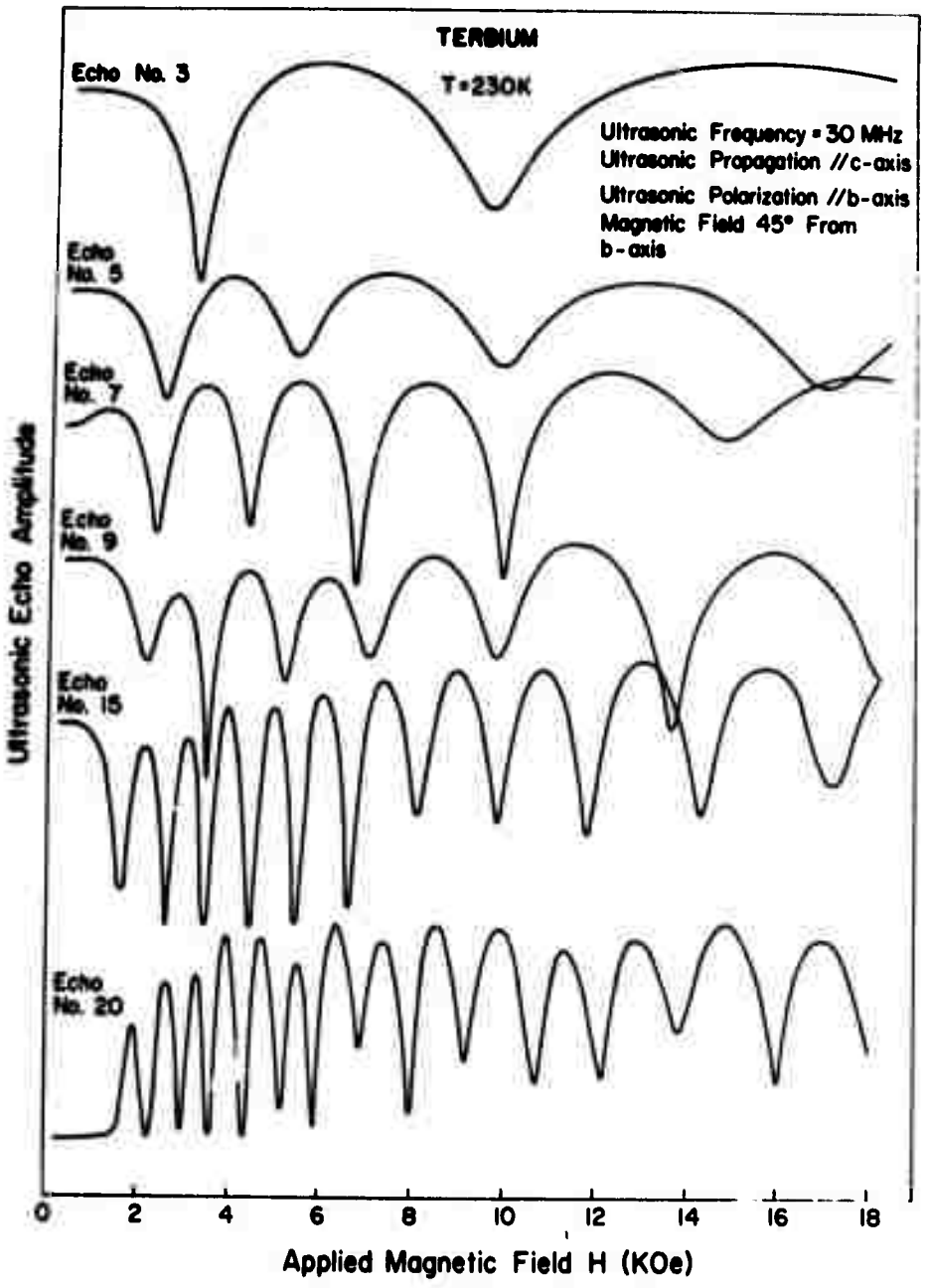

Fig. 2 Oscillations in elastic-wave amplitude as a function of the applied magnetic field in a terbium single crystal.

echoes from the third to the twentieth echo. The minima in the observed oscillations occur when the polarization of the echo returning to the transducer has been changed by the birefringence effect so that it is linear, but perpendicular to the direction in which the transducer can detect it piezoelectrically. It can be seen in Fig. 2 that the period of the oscillations increases with increasing magnetic field, as expected theoretically. Furthermore, the period of the oscillations and the field at which the oscillations are first observable decreases as the echo number increases. The data are interpreted through the assumption that the difference in the relative phase angle for waves whose polarization components lie along and perpendicular to the magnetization changes by the value π between successive maxima or successive minima of the amplitude oscillations.

The effect of temperature on the amplitude oscillations is shown in Fig. 3, in which the magnetic-field dependence of the amplitude of echo number 7 is displayed at temperatures between 235K and 210K. Actually, oscillations could be observed at temperatures as high as 250K, but they were not sufficiently strong or well resolved to permit quantitative measurements. Furthermore, no measurements could be made at temperatures below 200K, where the elastic-wave attenuation due to other sources was large, possibly screening the effects of magnetoacoustic birefringence.

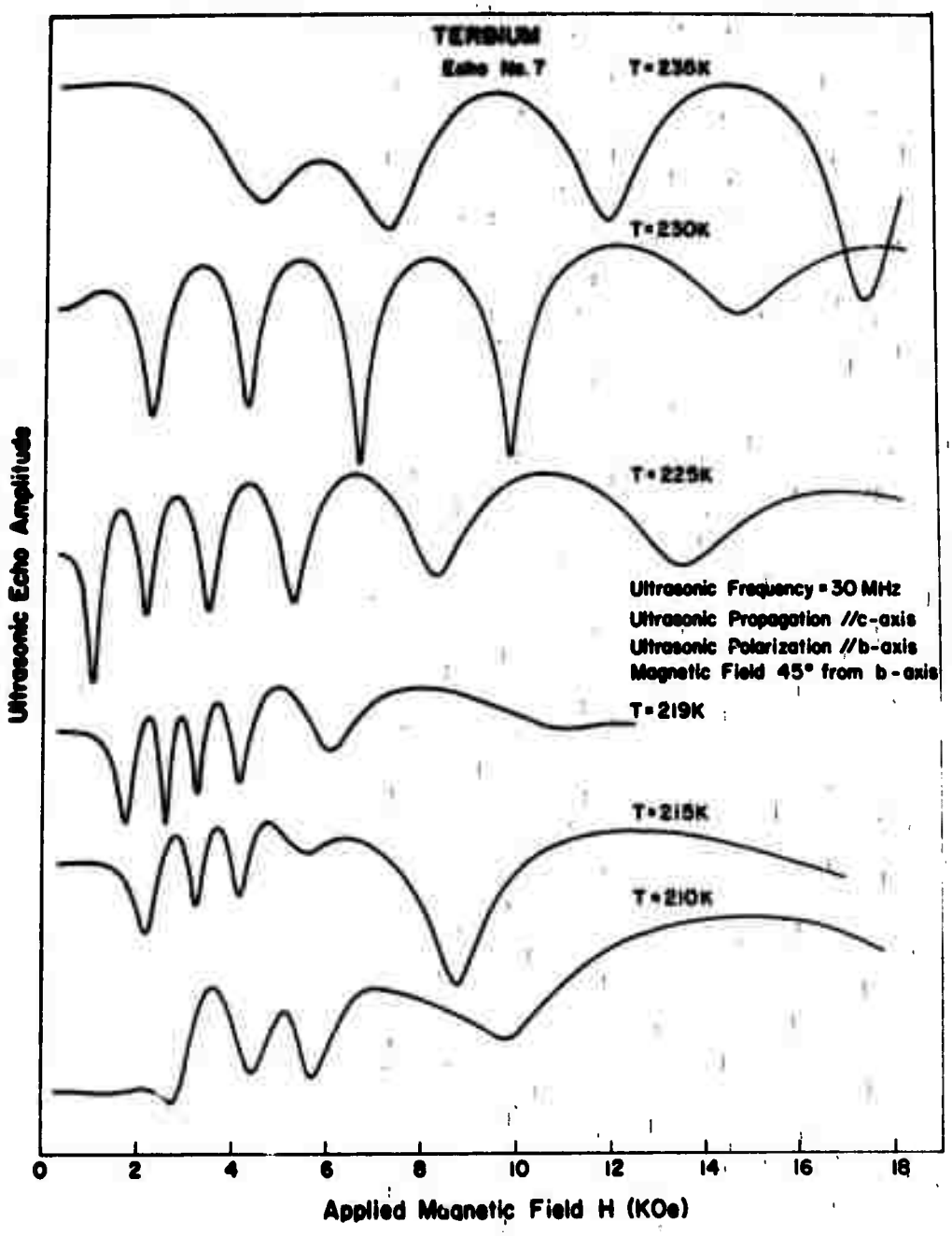

Fig. 3 Oscillations in the elastic-wave amplitude in a terbium single crystal as a function of temperature and applied magnetic field.

In general, the period of the oscillations decreased as the temperature was reduced, and, below the ferromagnetic-ordering temperature, T_C = 221K, their amplitude decreased while the initial field at which the oscillations were observed increased. In this temperature range, below T_C, few oscillations were observed, and, although this effect is not completely understood, it is possibly due to the strong remanent magnetization of terbium below its Curie temperature.

Through a determination of the magnetic field values at which successive maxima and minima of the amplitude oscillations occur, the dependence of the relative phase angle between different polarization components per unit length of travel, $\emptyset/\ell$, upon the applied field can be calculated. The values of $\emptyset/\ell$ obtained using data from all echoes at three different temperatures are shown in Fig. 4. For clarity, only the curves for temperatures of 230K, 225K, and 210K, are shown, although curves were also obtained for temperatures of 240K, 235K, 219K, and 215K. The solid curves represent the fitting of the experimental results to the formula expressed in Eq. (5), and the values of C_1 and C_2 obtained from this curve fitting are indicated in the insert table of Fig. 4. Both C_1 and C_2 decrease as the temperature is reduced.

The shear magnetoelastic coupling constant was calculated using the values of C_1 and values for ρ, M, and v obtained from the

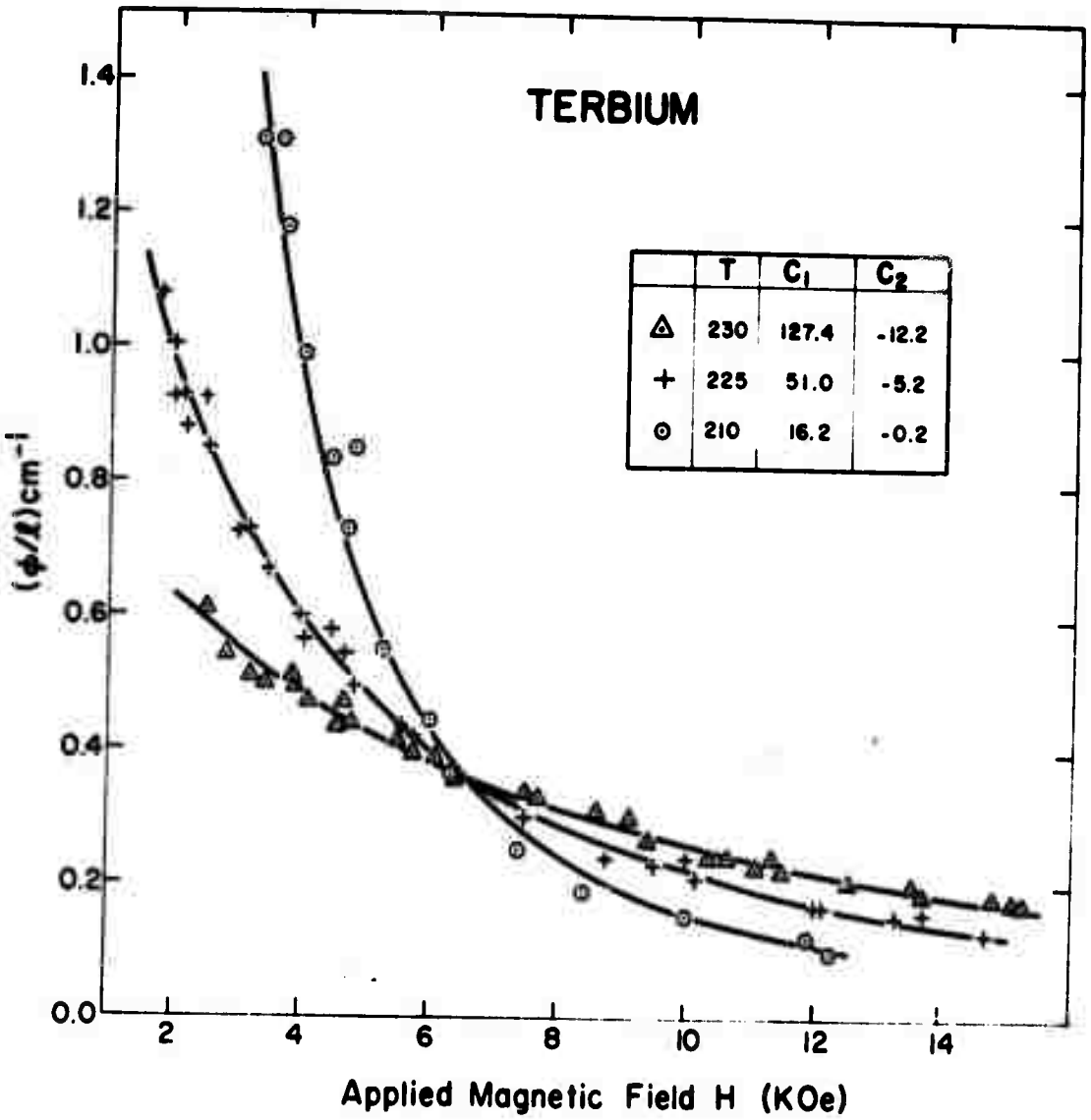

Fig. 4 Phase angle per unit length as a function of the applied magnetic field in a terbium single crystal at various temperatures.

literature[4,19,20]. The value of this coupling constant, b, is plotted as a function of temperature in Fig. 5. At a temperature of 240K the value of b is found to be 3.2×10^8 erg/cm^3, and it decreases linearly with decreasing temperature to a value of 1.6×10^8 erg/cm^3 at 225K. Below this temperature, the value of b decreases only slightly as the temperature is further decreased, reaching the value of 1.0×10^8 erg/cm^3 at 210K.

The only direct measurement of the shear magnetoelastic coupling in the heavy rare earths which has been previously reported is that of Clark, Bozorth, and DeSavage[5], who directly measured by means of strain gauges the shear magnetostriction in dysprosium single crystals above the magnetic-ordering temperature. The quantity which they measured, denoted $\lambda^{\epsilon,2}$, appeared, over the limited temperature range for which it was measured, to obey the temperature dependence predicted by Callen and Callen[21], leading Clark *et al.* to the extrapolated value for $\lambda^{\epsilon,2}$ at a temperature of 0K of 5×10^{-3}. Pollina and Lüthi[22], using the measured ratio of the shear magnetostriction to the longitudinal magnetostriction obtained by Clark *et al.*[5], $\lambda^{\epsilon,2}/\lambda^{\gamma,2} = 0.6$, and assuming the same ratio for terbium, estimated the shear magnetoelastic coupling constant for terbium at a temperature of 0K through the relationship $b = c_{44}\lambda^{\epsilon,2}$. The value that they obtained was 1.28×10^9 erg/cm^3. Using this estimate, and applying the temperature dependence pre-

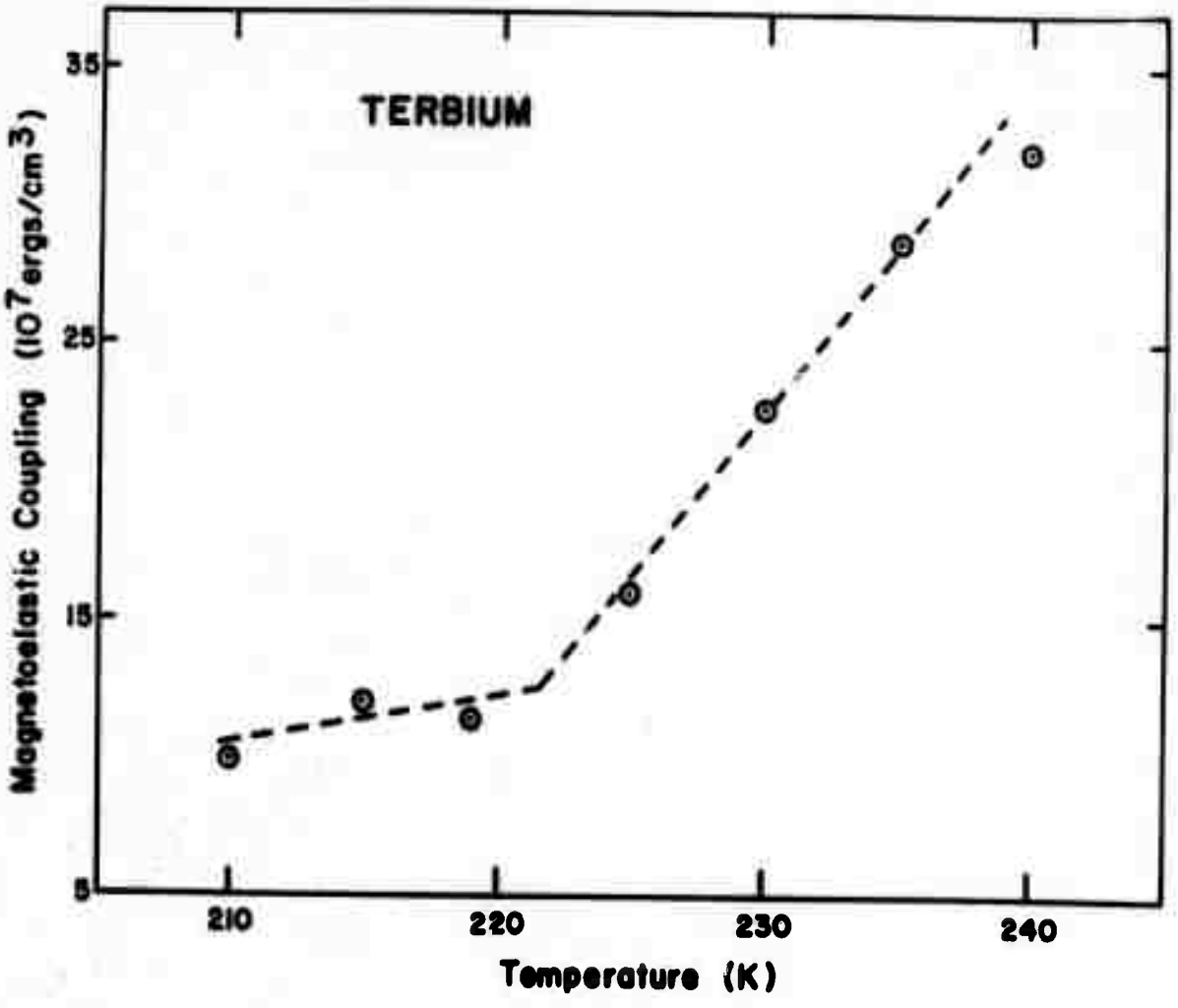

Fig. 5 Temperature dependence of the shear magnetoelastic constant in a terbium single crystal.

dicted by Callen and Callen[21], which agrees with that observed by Clark et al.[5], a value for b at the Curie temperature for terbium, T = 221K, can be obtained, with the result that $b = 2.3 \times 10^8$ erg/cm^3 at this temperature. This value is approximately twice the value obtained experimentally by the method reported here, but the agreement can be considered reasonable in view of the several approximations and extrapolations described above.

The most serious disagreement between the present method for the determination of the shear magnetoelastic coupling and other theoretical and experimental determinations of magnetoelastic effects in the rare earths lies in the temperature dependence of the constant b obtained in this work. In the results reported here, the constant b decreases with decreasing temperature, whereas the theory of magnetostriction due to Callen and Callen[21] and virtually all previous measurements of magnetostriction in the rare earths[5] agree that the magnetoelastic coupling increases with decreasing temperature. This discrepancy is examined further in Section IV of this report, in which a theoretical treatment of dynamic magnetoelastic effects is developed using a somewhat different approach from that of Schlömann[10].

Despite the discrepancies between the present interpretation of the experimental results and other work on magnetoelastic effects in the rare earths, which are expected to be eliminated as a better

theoretical treatment is developed, it is nevertheless extremely interesting to observe once again, from a purely phenomenological point of view, the experimental results presented in Figs. 2 and 3. It can be seen that, through the proper choice of temperature and applied magnetic field strength, a given ultrasonic echo can be reduced essentially to zero amplitude because of the magneto-acoustic birefringence. This effect is exactly analogous to that utilized in certain types of microwave isolators, the so-called "gyrators." One can easily envision a new class of nonreciprocal acoustic devices of this type which may be quite useful in communications and signal-processing applications.

2. The Effect of a Magnetic Field on Anomalous Ultrasonic Attenuation in Polycrystalline Terbium

Ultrasonic Attenuation in magnetic materials in the vicinity of magnetic phase transitions has met with great interest recently. The research carried out in this area has been reviewed in papers by Garland[23] and by Lüthi, Moran, and Pollina[24]. Experiments on single crystals of the heavy rare earths[1,3,22] all show a pronounced increase in the ultrasonic attenuation of longitudinal waves in the paramagnetic phase as the Neel temperature, T_N, is approached. Below T_N the attenuation decreases sharply, so that there is a sharp attenuation peak at T_N. In single-crystal terbium, however,

because the Curie temperature, T_C, is only 7K below T_N, the attenuation levels off at T_N and then rises slowly until T_C is reached. Analysis of these single-crystal results has shown that the temperature dependence of the critical attenuation has the form

$$\Delta\alpha_{\ell}(q,\varepsilon) = Bq^2\varepsilon^{-\eta} , \qquad (1)$$

where B is a temperature-independent constant, q is the ultrasonic wave vector, ε is the reduced temperature $(T-T_N)/T_N$, and η is a critical index which characterizes the magnetic behavior of the material.

Several theories have been developed[25-27] in an attempt to describe this anomalous peak in the attenuation at the Néel temperature. The basic physical idea underlying all these theories is the perturbation of an elastic wave by the thermal fluctuations of the local magnetic moment of the material when there is a significant spin-lattice coupling. As the phase transition is approached, the fluctuations will increase rapidly, leading to a rapid increase in elastic-wave attenuation. The first theoretical approach to this problem was that of Tani and Mori[25], who calculated the net rate of change of phonon population (rate of annihilation less rate of creation) by using an interaction Hamiltonian with volume magnetostrictive coupling. The ultrasonic attenuation was

found to be proportional to the double Fourier transform of a four-spin correlation function. They then determined the four-spin correlation function by assuming that it can be factored into the product of two two-spin correlation functions, which can then be evaluated in the hydrodynamic limit $\omega\tau << 1$, where ω is the ultrasonic angular frequency and τ is the spin relaxation time. Kawasaki[26] used scaling-law arguments to determine the four-spin time-independent correlation function, whereas Laramore and Kadanoff[27] used a mode-mode coupling theory[28]. Physically this theory corresponds to the absorption of a phonon simultaneously with the creation of two spin fluctuations.

Despite the differences in these theories, the temperature dependence of longitudinal ultrasonic attenuation in the vicinity of a magnetic phase transition is described by all of the theories by a relationship similar to that of Eq. (1). The values of the exponent, η, predicted by these different theories, however, differ widely. For an anisotropic antiferromagnet, for example, values for the exponent of 3/2 or 4/3 are obtained, depending upon the theoretical treatment[24]. For an isotropic antiferromagnet, the corresponding theoretical predictions are 5/3 and 1. Ultrasonic measurements on terbium single crystals[1,3,22] using longitudinal waves propagated along the hexagonal axis yielded $\eta = 1.24 \pm 0.1$[22] or $\eta = 1.45 \pm 0.2$[1,2].

Few measurements have been made on the effect of an applied magnetic field on the critical attenuation of longitudinal ultrasonic waves near a magnetic phase transition[1,3]. Belov et al.[29] have treated this effect in terms of the Landau approach to second-order lambda-type transitions[30], and they showed that the field dependence could be attributed to the dependence of the relaxation time, τ, which they found to decrease with increasing magnetic field. In particular, they showed that $\tau \propto H^{-2/3}$ near the magnetic-ordering temperature.

The present report describes the temperature dependence of the longitudinal ultrasonic attenuation in the vicinity of magnetic phase transitions in polycrystalline terbium and the effect of an applied magnetic field on this attenuation. The temperature dependence of the attenuation is interpreted here in terms of the theory of Laramore and Kadanoff[27], and the field-dependence of the attenuation is interpreted in terms of the predictions of Belov et al.[29]

The high-purity polycrystalline terbium specimen used in this work was obtained from Research Chemicals, Inc., Phoenix, Arizona; the stated purity was 99.85%, with the impurities consisting largely of other rare earths. A cylinder was prepared, 6 mm in diameter and 10 mm in length, with flat, parallel surfaces perpendicular to the cylindrical axis. Spark-machining techniques were used in the

preparation of the sample, which was etched and electropolished[31] after spark machining in order to remove cold-worked layers.

An X-cut quartz transducer of fundamental frequency 10 MHz was bonded to the specimen with Dow-Corning V-9 silicone material, and ultrasonic pulse-echo measurements were made with the Matec, Inc. apparatus described above. A magnetic field as large as 15 kOe was applied in the plane perpendicular to the cylindrical axis of the specimen, and the ultrasonic attenuation was recorded at constant temperature as a function of the applied field strength. All measurements were made when the magnetic field was increasing, in order to obtain reproducible results in the presence of normal magnetic hysteresis. In polycrystalline terbium, the attenuation was so large that it was normally possible to use only the first two ultrasonic echoes for the attenuation measurements. The temperature measurement and control system was identical to that described above.

The temperature dependence of the longitudinal ultrasonic attenuation in polycrystalline terbium at 10 MHz is shown in Fig. 6. The attenuation at room temperature was 3.4 db/cm, somewhat larger than that obtained by Rosen[32], who found a value of 2.7 db/cm at the same temperature. This difference is perhaps due to the different impurity content of the two specimens. Below room temperature, the attenuation remained constant down to 270K,

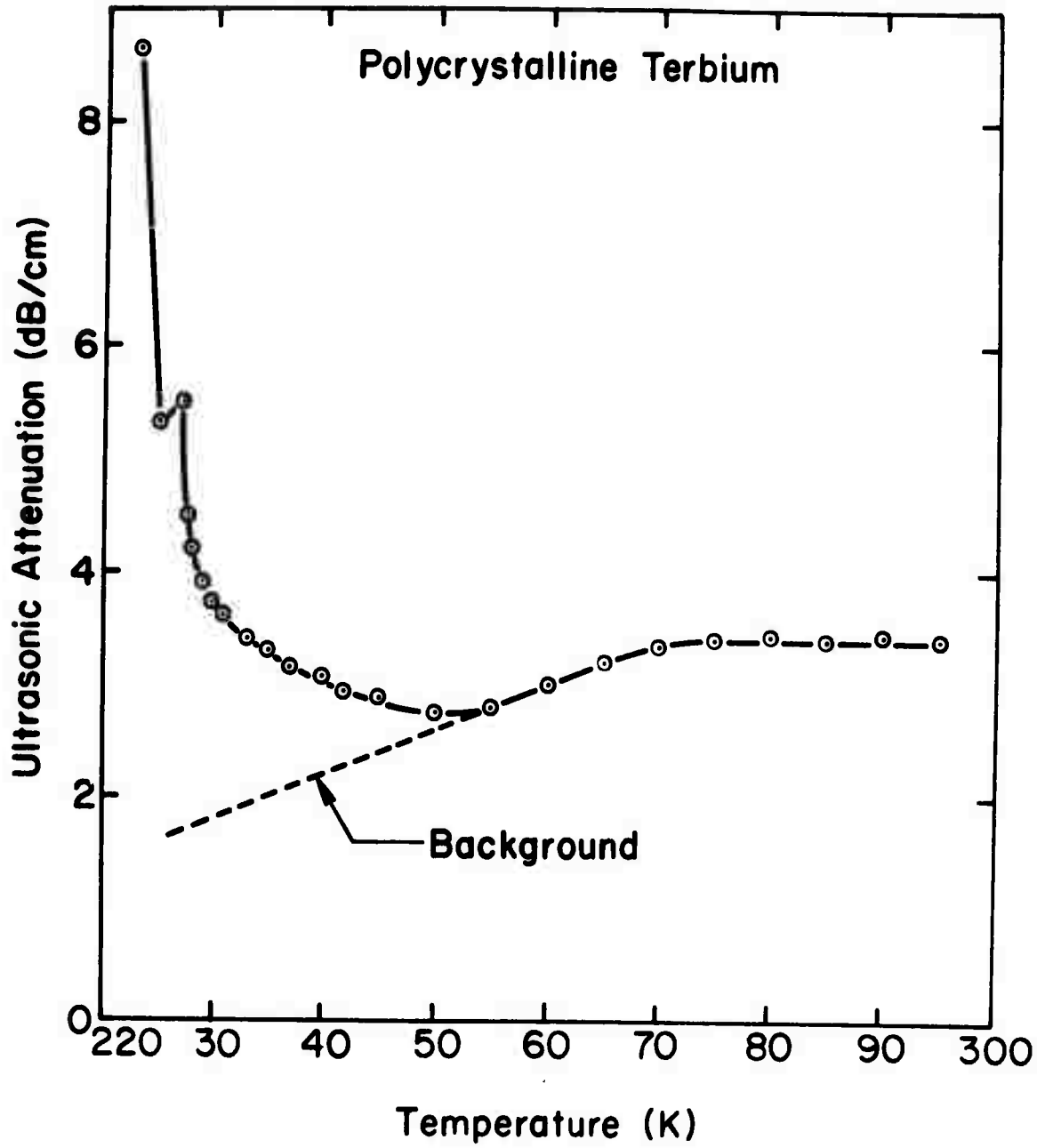

Fig. 6 Temperature dependence of the longitudinal ultrasonic attenuation in polycrystalline terbium in zero applied magnetic field.

and it then began to decrease almost linearly with decreasing temperature, reaching a broad minimum at a temperature of 250K. With a further decrease in the temperature, the attenuation began to increase, slowly at first, and then rather sharply as the Neel temperature was approached. A peak in the attenuation was reached at T_N, with a slight reduction in attenuation just below T_N, followed by a very rapid increase in the attenuation as the temperature was lowered further toward T_C. In fact, the entire ultrasonic echo pattern disappeared at a temperature of 219K, and no quantitative measurements could be made below 221K.

The effect of an applied magnetic field on the temperature dependence of the longitudinal attenuation is shown in Fig. 7. In the presence of an applied field, the attenuation peak was shifted to higher temperatures, broadened, and reduced in amplitude. Also in high magnetic fields, the minimum in the attenuation at a temperature of approximately 225K was enhanced greatly, exhibiting a cusplike behavior apparently associated with the helimagnetic-ferromagnetic transition. Even with the application of a magnetic field, the attenuation at temperatures below 221K was too large to permit quantitative measurements. These results are similar in most respects to those obtained with single-crystal specimens of terbium[1,3] and those obtained by Belov et al.[29] with the alloy Elinvar (Fe-Ni-Cr). The dashed line in Figs. 6 and 7 represents

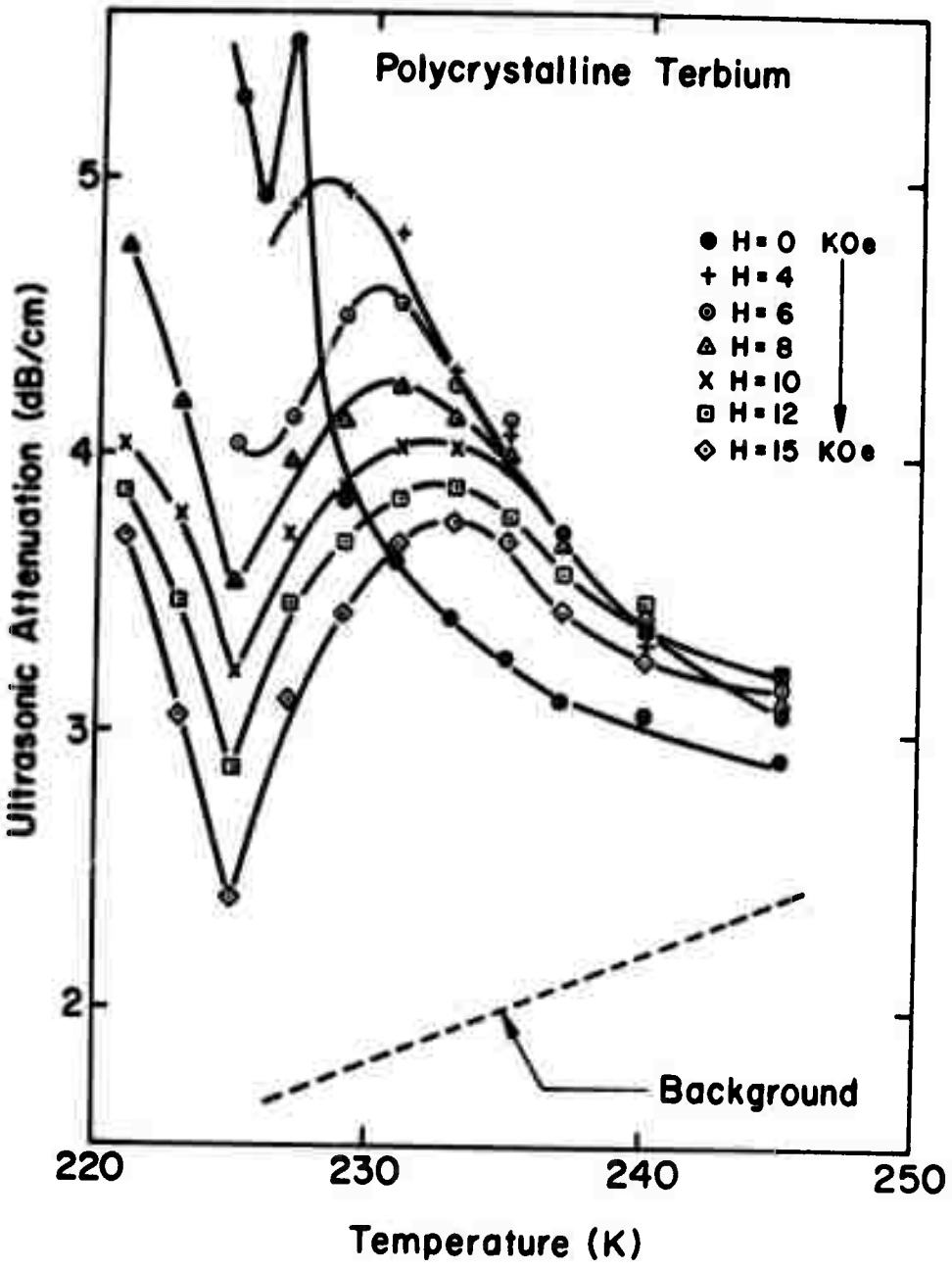

Fig. 7 The effect of an applied magnetic field on the temperature dependence of longitudinal ultrasonic attenuation in polycrystalline terbium.

the background attenuation due to sources of nonmagnetic character and is obtained by extrapolation from the linear decrease in attenuation with decreasing temperature above 255K.

The temperature dependence of the ultrasonic attenuation in the paramagnetic phase was analyzed according to Eq. (1). In Fig. 8 is shown a plot of the logarithm of the attenuation, $\Delta\alpha$, as a function of the logarithm of the temperature increment $T-T_p$, where T_p is the temperature at which the peak attenuation occurs. The data points indicate that there are two inverse power laws which describe the critical attenuation. One law, with a small value of the exponent, η_ℓ, dominates over the temperature range $\epsilon \leq 0.03$, and the other law, with a larger value of the exponent, η_h, dominates the behavior over the range $0.03 \leq \epsilon \leq 0.06$. The values of the exponents at various applied magnetic-field values are listed in Table I. At zero applied field, the values of η_h and η_ℓ are, respectively, 0.77 and 0.30. The application of a magnetic field of strength 4 kOe increases the larger exponent to a value of 1.05, but a further increase in the field leads to a decrease in the value of the exponent. The value of the smaller of the two exponents decreased with increasing magnetic field, reaching a broad minimum in the vicinity of 10 kOe, but then increasing slightly at 15 kOe.

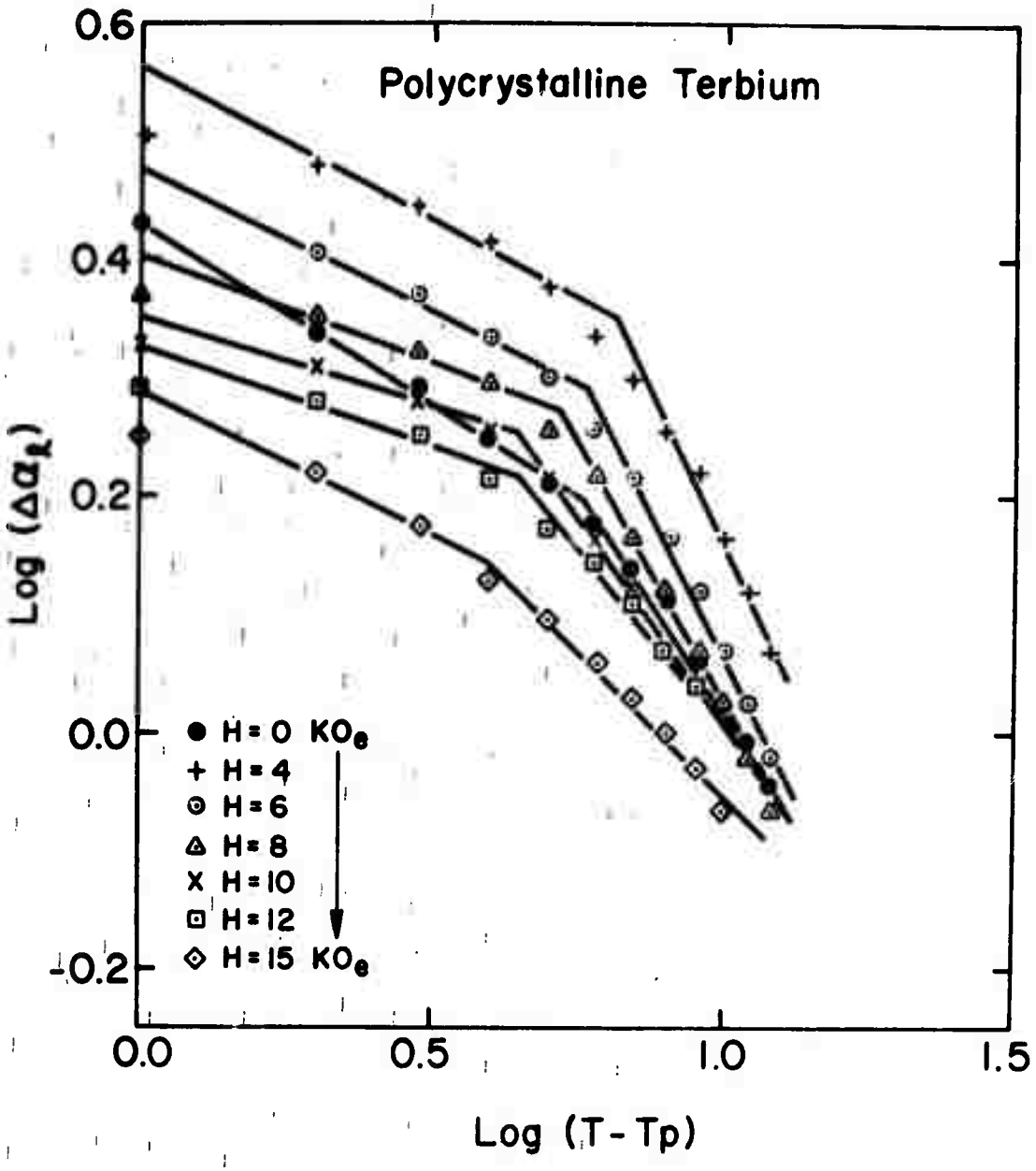

Fig. 8 Log-log plot of the critical ultrasonic attenuation as a function of temperature in polycrystalline terbium at various field values. The field is perpendicular to the propagation direction.

TABLE I

Values of the Critical Exponents η_h and η_ℓ at Various Applied Magnetic Fields H

H (kOe)	η_h	η_ℓ
0.0	0.77	0.30
4.0	1.05	0.27
6.0	0.95	0.24
8.0	0.83	0.19
10.0	0.72	0.16
12.0	0.63	0.17
15.0	0.50	0.24

According to Laramore and Kadanoff[27], Eq. (1) can be written in the form

$$\Delta\alpha_\ell \propto Bq^2\epsilon^{+\alpha}/S_\sigma^* , \qquad (2)$$

where the exponent, α, is the critical index which describes the divergence of the magnetic portion of the specific heat C_p in zero applied magnetic field, and S_σ^* is the relaxation rate of the spin fluctuations. Thus, in this form for the theoretical expression for the attenuation, the temperature dependence of the critical attenuation is confined to the spin-fluctuation rate, since the critical exponent, α, is small in the theory of Laramore and Kadanoff. Since Belov *et al.*[29] found the spin relaxation time τ near the magnetic phase transition to be proportional to $H^{-2/3}$, the field dependence of the peak attenuation, as shown in Fig. 7, should decrease with increasing field as $H^{-2/3}$ also.

A plot of the logarithm of the critical attenuation at the peak, $(\Delta\alpha_\ell)_{max}$, as a function of the logarithm of the applied magnetic field, H, is shown in Fig. 9. The slope of the straight line log-log plot is, however, -1/2, rather than the predicted value of -2/3. This difference between theory and experiment may have various causes. One possibility is the dependence as ϵ^α, which has been ignored in the preceding analysis because the exponent is presumed to be small, which may itself exhibit a field dependence.

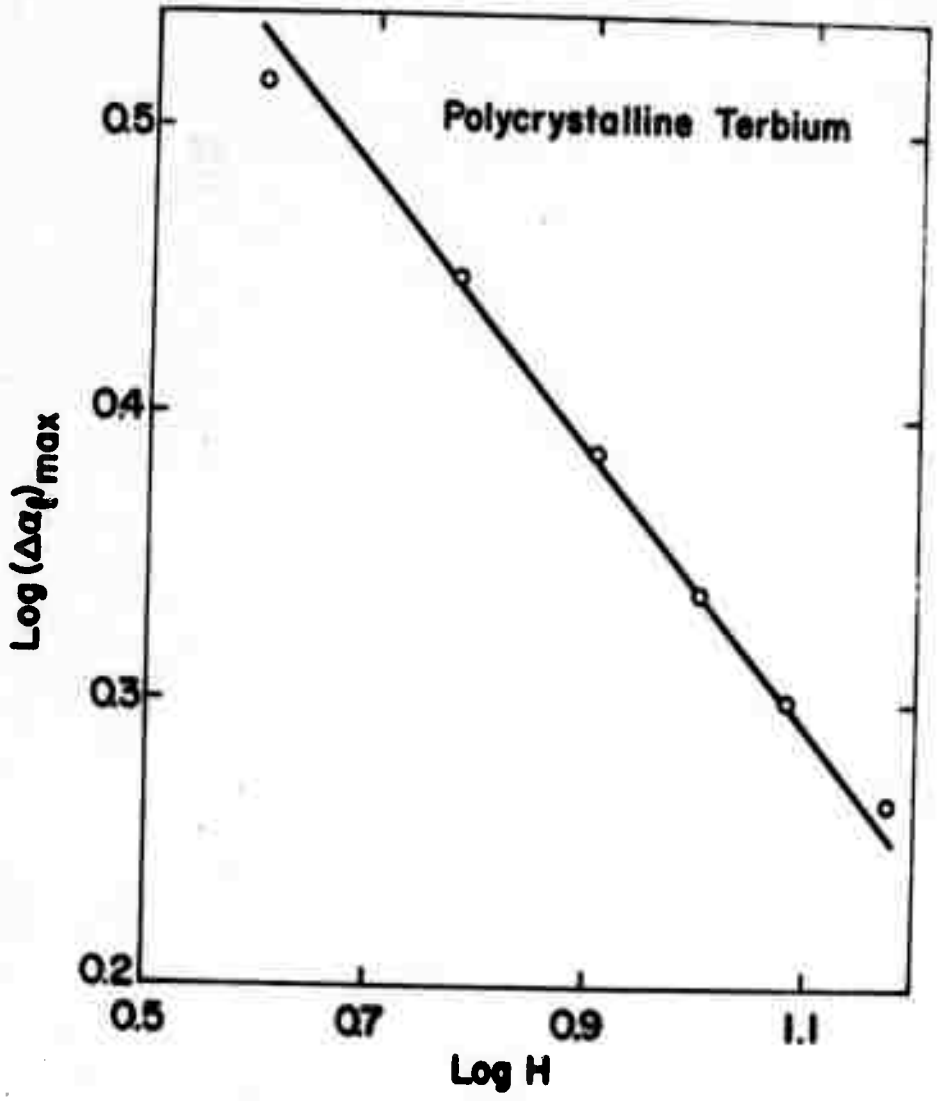

Fig. 9 Log-log plot of the maximum critical attenuation as a function of applied magnetic field. The slope of the straight line is -1/2.

There have been several suggestions to explain the two power-law regions observed in the present work, as well as in investigations of other antiferromagnetic materials. Measurements on single crystals of the heavy rare earths[1,3,22] have shown that only one power law can represent the temperature dependence of the attenuation in zero applied field. The corresponding critical exponents of this power-law dependence for single crystals agree with the theoretical predictions[26,27]. It has been found, however, that when a magnetic field is applied, the single power law breaks into two power-law regions, with one critical exponent equal to that which is found at $H = 0$, valid for the region $0.04 \leq \epsilon \leq 0.11$. The other power-law exponent, approximately one-quarter the value of the first, provides the dominant behavior in the region $0.01 \leq \epsilon \leq 0.04$.

For isotropic antiferromagnetic materials, Laramore and Kadanoff[27] predict that $\Delta\alpha_\ell \propto \epsilon^{-1+3\alpha/2}$, where $\alpha \leq 0.16$. If polycrystalline terbium is assumed to be essentially an isotropic antiferromagnet, the critical exponent is expected to be in the range $0.76 \leq \eta \leq 1.0$, in good agreement with the value $\eta_h = 0.77$ obtained experimentally at zero applied magnetic field. The low-temperature critical exponent, $\eta_\ell = 0.3$, is difficult to explain in terms of the existing theories. However, calculations based on energy-density coupling[33] seem to indicate that for an isotropic antiferromagnet it is possible to find that $\Delta\alpha_\ell \propto \epsilon^{-1/3}$.

The decrease in the measured high-temperature critical exponent, η_h, with applied magnetic field may be explained in terms of the field dependence of the relaxation rate, S_σ^*, of Eq. (2). Again, if it is assumed that polycrystalline terbium can be regarded as an isotropic antiferromagnet and that the spin-fluctuation relaxation rate is[27]

$$S_\sigma^* \propto \varepsilon^{(1-\alpha/2)} \propto \varepsilon^{(\eta_h+2)/3}, \qquad (3)$$

then the substitution of $S_\sigma^* \propto H^{-2/3}$ into Eq. (3) gives

$$\varepsilon^{(\eta_h+2)/3} \propto H^{2/3}. \qquad (4)$$

The relationship expressed in Eq. (4) indicates that a plot of the quantity $(\eta_h+2)/3$ *vs.* log H should be linear, with a slope equal to $2/(3\log \varepsilon)$. This plot is shown in Fig. 10, using the values for η_h listed in Table I. The relationship is indeed a straight line, whose slope is equal to - 0.39. This value gives $\varepsilon = 0.02$, or $T-T_p = 4.6$K. It can be seen from Fig. 8 that the values of $T-T_p$ at which η_h begins to be dominant range between 6.5K at H = 4 kOe and 4.0K at H = 15 kOe.

From the results described above, the following conclusions may be drawn:

a. The results shown in Fig. 7 indicate that the ultrasonic attenuation in polycrystalline terbium exhibits a maximum which

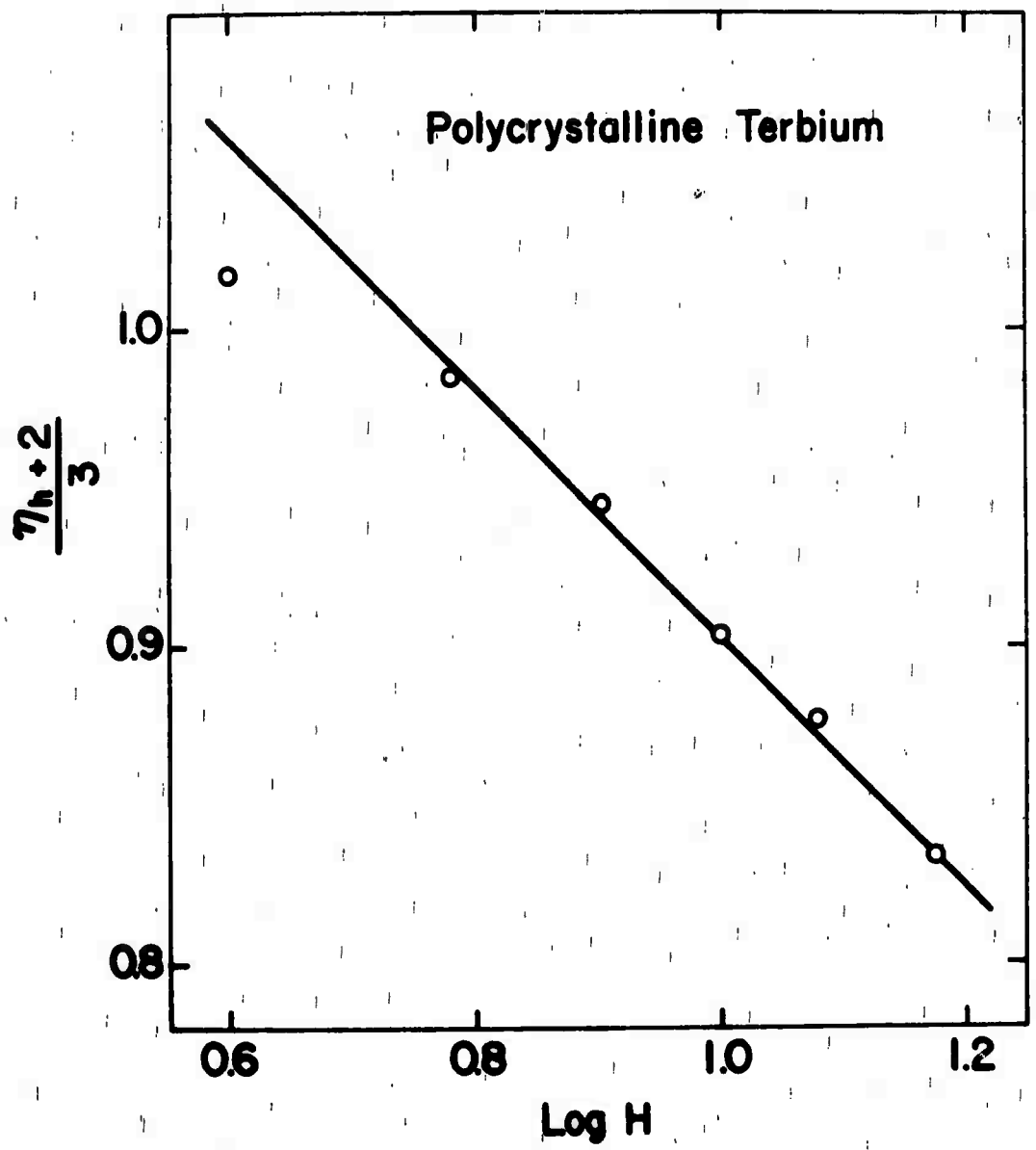

Fig. 10 Plot of the quantity $[(\eta_h + 2)/3]$ as a function of log(H).

occurs in the temperature range between 228K and 233K, depending upon the value of the applied magnetic field strength. This suggests that, if polycrystalline terbium is to be used for magnetostrictive ultrasonic generation in the megahertz range, the intensity of the waves generated will be greatly influenced by the attenuation of the sample itself in this temperature range. The attenuation exhibits a minimum at a temperature of 225K, and ultrasonic generation at this temperature would perhaps be enhanced with respect to that obtained at other temperatures.

b. In the presence of an applied magnetic field or in zero applied field, the attenuation can be represented by two power laws with two critical exponents, each being dominant over a temperature range of approximately 6K.

c. At zero applied field, the high-temperature exponent is equal to 0.77, agreeing with the prediction of Laramore and Kadanoff for isotropic antiferromagnets. The low-temperature exponent is 0.30.

d. Under the influence of an applied magnetic field, the ultrasonic attenuation peak shifts toward higher temperatures. The magnitude of the attenuation at the peak was found to be proportional to $H^{-1/2}$.

e. The analysis of the high-temperature critical exponent as a function of applied magnetic field gives support both to the theory of Laramore and Kadanoff and to that of Belov _et al_. This

support for these theories is based upon the assumption that polycrystalline terbium represents a reasonable approximation to an isotropic antiferromagnet over the temperature range under consideration.

III. MAGNETOSTRICTIVE ELASTIC-WAVE GENERATION IN RARE-EARTH METALS AND COMPOUNDS

The principal goal of the research program described in this report is the development of highly efficient elastic-wave transducers based upon the utilization of the extremely large magnetostriction exhibited by many pure rare-earth metals and their alloys and by certain intermetallic compounds of the rare earths with iron-group elements. Magnetostrictive ultrasonic transducers have largely been employed for high-power ultrasonic generation at frequencies in the range below 100 kHz, and in most applications they have been fabricated from various iron-group alloys or from ferrite-type ceramics[34]. Although there is considerable potential for the application of certain rare-earth materials in this frequency range, the work described here has been concentrated on the development of transducers for operation at much higher frequency, in the range above 100 MHz. The research previously carried out in this program has been centered on the pure rare earths, mainly in the form of thin films deposited on nonmagnetic substrates such as quartz and sapphire[1]. The pure rare earths have the disadvantage, however, that they exhibit large magnetostriction only at the cryogenic temperatures at which they become magnetically ordered. This restriction to operation only at low

temperatures would certainly limit the range of applications for which transducers fabricated of these materials might be employed. Thus, the research which has been carried out under this program has been primarily directed toward the development of a better fundamental understanding of the mechanisms of dynamic magnetostrictive effects in these pure rare-earth elements. The recent discovery, however, by Clark and Belson[2] of extremely large magnetostriction in polycrystalline terbium-iron compounds at room temperature and above has opened a new range of materials for investigation in this program. Specimens of the intermetallic compound, $TbFe_2$, have been obtained for use in this program, and it has been shown that strong elastic-wave generation can be induced in this compound at temperatures as high as 350K and at frequencies as high as 1.35 GHz. This work, together with further studies of magnetostrictive elastic-wave generation in this films of dysprosium and terbium, is the subject of this section of this report.

1. Thin-Film Preparation

Since the same general technique was employed for the preparation of thin films of all the materials investigated in the work reported here, and since the purity, thickness, and other film characteristics are very important in the determination of the

magnetostrictive properties of the polycrystalline films used in this work, the following brief description of the procedures used for film deposition is in order.

The films used in this work were deposited onto substrates of single-crystal quartz or sapphire by means of evaporation from a resistive heater in high vacuum. In the case of the pure rare earths, the bulk material to be evaporated could be placed in direct contact with the resistance heater, which was fabricated either of tungsten or tantalum. In the case of the terbium-iron compound, however, the amalgamation of the iron constituent with the heater material which occurs at high temperature required the use of a boron-nitride crucible in order to prevent direct contact of the evaporant with the heater. In the latter case, better results can probably be obtained through the use of an induction-heating system, but such a method has not yet been attempted.

Prior to film deposition the substrates were cleaned in a multistage process involving the use of nitric acid, organic solvents such as acetone, hexane, and methanol, and standard laboratory detergents, with agitation in an ultrasonic cleaner. After evacuation of the bell-jar system to a pressure of approximately 10^{-7} Torr, the substrate was heated to a temperature of approximately 300C and maintained at this temperature during the evaporation. As in the case of nickel and permalloy films[34], the elevated

temperature of the substrate assures good adhesion of the film to the substrate. With a shutter covering the substrate, the evaporant was brought to the melting point and outgassed until the system pressure returned to a value near its initial value. The shutter was then opened, and the film was deposited as rapidly as possible. Immediately after deposition, the film was coated with a protective layer of silicon monoxide of thickness 0.1 μm.

For most of the work reported here, the thickness of the film was estimated from geometrical considerations, based on the mass of the evaporant. Although this method is not accurate to better than 25 per cent, it was adequate for the preliminary results presented here. The recent acquisition of a quartz-crystal deposition-thickness monitor will permit much more accurate determinations of the thickness of films to be deposited in future work. Films of the order of 1-2 μm in thickness were normally deposited, although the results of the preliminary measurements reported here indicate the necessity of films of thickness perhaps as large as 5 μm in order to obtain efficient transducer operation.

The characteristics of films produced following the procedures described above were reasonable reproducible. In fact, any lack of reproducibility was apparently due as much to the variation of the quality of the substrates used from one evaporation to the next as to any other single factor. With regard to the use of silicon

monoxide for the protection of film surfaces against oxidation or other contamination, it appears that this method provides sufficient protection to prevent degradation of transducer efficiency over a period of time of the order of five years. Without such passivation, a film becomes totally useless as a transducer within hours after its deposition.

2. Elastic-Wave Generation in Terbium-Iron Thin Films

In a recent paper Clark and Belson[2] reported the observation of extremely large room-temperature magnetostriction in polycrystalline specimens of terbium-iron compounds, primarily in $TbFe_2$, in which the magnetostrictive strain was measured to be 2500×10^{-6}. This is in strong contrast to most iron-group materials, for which room-temperature magnetostriction values of 40×10^{-6} are typical, and it is even large compared to any polycrystalline pure rare earth, even at low temperatures. In fact, the observed magnetostriction for polycrystalline $TbFe_2$ at room temperature is comparable to that observed in single-crystal dysprosium, terbium, and holmium at very low temperatures. Clark and Belson also predicted the existence of very large magnetostriction in other rare-earth-iron compounds, using the theory of Tsuya *et al.*[35] It is, of course, well known that many iron-group materials find useful applications as low-frequency magnetostrictive transducers[36]. The potential applications

for these new compounds, which exhibit magnetostriction hundreds of times larger than that of iron-group materials should be numerous.

In the research reported here, elastic-wave generation in thin films of terbium-iron compounds has been studied at temperatures between 4.2K and 350K, and at frequencies of 690 MHz and 1.35 GHz. The film thickness was between 1 and 2 μm in all cases, and the films were prepared according to the method outlined in Section III.1. The bulk specimen from which the films were evaporated was prepared by Research Chemicals, Inc., Phoenix, Arizona. According to the vendor, the material was prepared by adding terbium metal to an alumina crucible containing molten iron, in a high-vacuum atmosphere. A slight excess (approximately 2 per cent) of terbium, over the correct stoichiometric quantity for $TbFe_2$, was added in an effort to take account of the higher vapor pressure of terbium. The final material, however, was approximately 8 per cent deficient in terbium, according to an analysis performed by the vendor. Thus, the starting material used for the preparation of transducer films was probably a mixture of $TbFe_2$, $TbFe_3$ (which also exhibits rather large static magnetostriction according to Clark and Belson[2]), and other terbium-iron phases, as well as small amounts of unknown impurities. Thus, in the following description of the experimental results obtained on elastic-wave generation in terbium-iron films, it must be realized that the films were composed

only partially of $TbFe_2$, with an unknown amount of other terbium-iron compounds, probably some free iron and terbium, and a small but unknown percentage of impurities of unknown composition. No attempt has yet been made to analyze the films used for elastic-wave generation, but it is expected that such an analysis will be carried out soon.

Measurements of elastic-wave generation were carried out at frequencies of 1.35 GHz and 690 MHz. At both frequencies the specimen was subjected to an applied magnetic field which was supplied by one of two magnets: A conventional iron-core electromagnet capable of fields as high as 18 kOe was used for the majority of the measurements; for higher fields, a superconducting solenoid capable of fields up to 50 kOe was employed. In both cases, the sample could be maintained at any desired temperature between 1.5K and 350K through the use of a continuous-flow helium cryostat and an electronic control system. In the case of the iron magnet, the field could be applied at any direction with respect to the plane of the terbium-iron film, but in the case of the superconducting magnet the field was always applied perpendicular to the plane of the film.

At 1.35 GHz the sample was placed inside a circularly cylindrical re-entrant resonant cavity, with the film parallel to the rf magnetic field at a position where this field was maximum.

At 690 MHz the sample was placed inside a flat stripline cavity, again with the film parallel to the rf magnetic field at the position where this field reached its maximum value. In the conventional magnet at both frequencies, the configuration was such that the rf magnetic field could be directed either parallel to or perpendicular to the applied steady field, but in the superconducting solenoid, the fields were always perpendicular to each other.

Substrates of both X-cut and AC-cut quartz were used for the films, primarily serving as delay lines in order to permit the observation of echoes of the magnetostrictively generated and detected elastic waves. All of the results reported here were obtained with the X-cut quartz substrates, which permitted the determination of the polarization of the elastic waves unambiguously. Because of the position of the sample films in the resonant cavities, piezoelectric generation of elastic waves was negligible. In future work, however, it is planned to use a two-cavity arrangement, in which elastic waves can be generated magnetostrictively and detected piezoelectrically, and vice versa.

In all cases, only transversely polarized elastic waves were generated with appreciable amplitude. Strong generation was observed when the applied magnetic field was perpendicular to the plane of the film and, hence, perpendicular to the rf magnetic field. With this configuration for the dc and rf fields, it would

be expected, under the assumption that the terbium-iron film behaves similarly to a simple isotropic ferromagnet or ferrimagnet, that a uniform-precession magnetic resonance would be excited in the film, accompanied by a precessing magnetostrictive strain. Such a strain, with longitudinal components in the plane of the film, would induce shear stresses at the surface of the substrate, leading to the generation of shear waves in the substrate. The resonance should occur, under the assumption of a simple isotropic ferromagnet, at a value of the applied dc magnetic field which satisfies the resonance condition,

$$\omega = g\mu_B H_i \ , \qquad (1)$$

where ω is the rf angular frequency, g is the Landé factor, presumably for the rare-earth ions, μ_B is the Bohr magneton, and H_i is the magnetic field within the film, equal to $H-4\pi M$, where M is the magnetization within the film. Thus, the resonance should be expected to occur, for the relatively low frequencies at which this experiment was performed, at a value of the applied dc field somewhat greater than $4\pi M$. Since the composition of the films used in this work was not accurately known, and since the magnetization was not measured in this work, the value of the field at which resonance would be expected could not be calculated with any accuracy.

Typical results for elastic-wave generation in a terbium-iron film at different temperatures are shown in Figs. 11-13, in which the dependence of elastic-wave generation at a frequency of 690 MHz on the applied dc magnetic field is shown. In Fig. 11 the field dependence of magnetostrictively generated shear elastic waves at a temperature of approximately 300K (room temperature) is shown. The resonant behavior at this temperature is clearly seen, with the peak intensity occurring at a field value of approximately 5 kOe. In Fig. 12, the field dependence of the elastic-wave intensity at a temperature of 200K is shown. Again, there is a clearly resonant behavior, with the maximum intensity occurring at a field of approximately 13.5 kOe, apparently reflecting the larger magnetization in the film at this temperature. In Fig. 13, the resonance has broadened considerably at a temperature of 100K, and the field at which maximum intensity occurs has increased to approximately 29 kOe. At temperatures below 100K, the maximum available magnetic field strength of 50 kOe was not sufficient to cover the full range of the resonant behavior, although the field at which maximum intensity occurred could be determined to temperatures as low as 50K. The field at which the maximum intensity occurred is illustrated as a function of temperature in Fig. 14 over the temperature range from 50K to 350K. It is believed that in all cases the elastic-wave generation which was observed was the

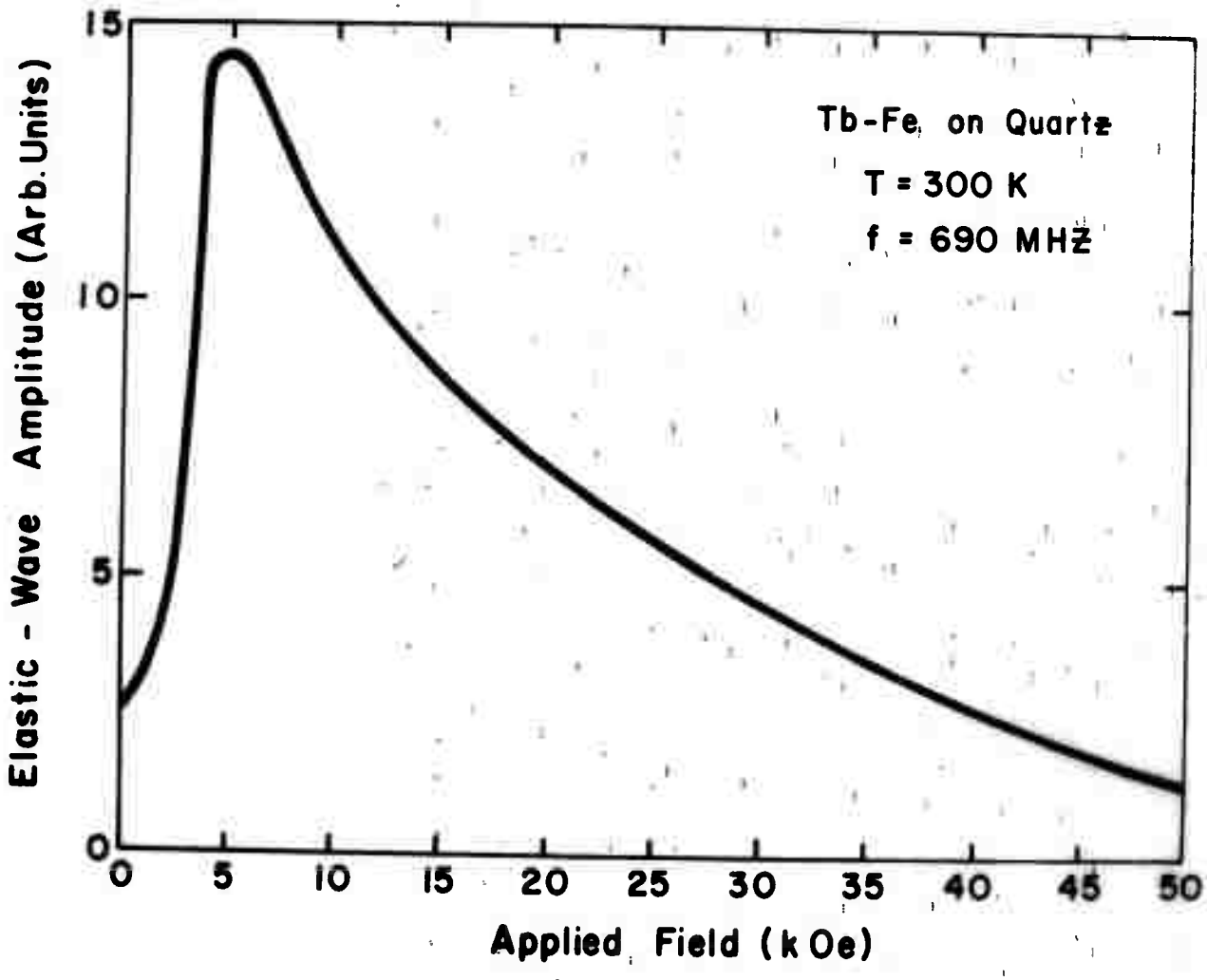

Fig. 11 Elastic-wave generation in a terbium-iron polycrystalline thin film as a function of applied magnetic field. The field is perpendicular to the plane of the film, and the temperature is 300 K.

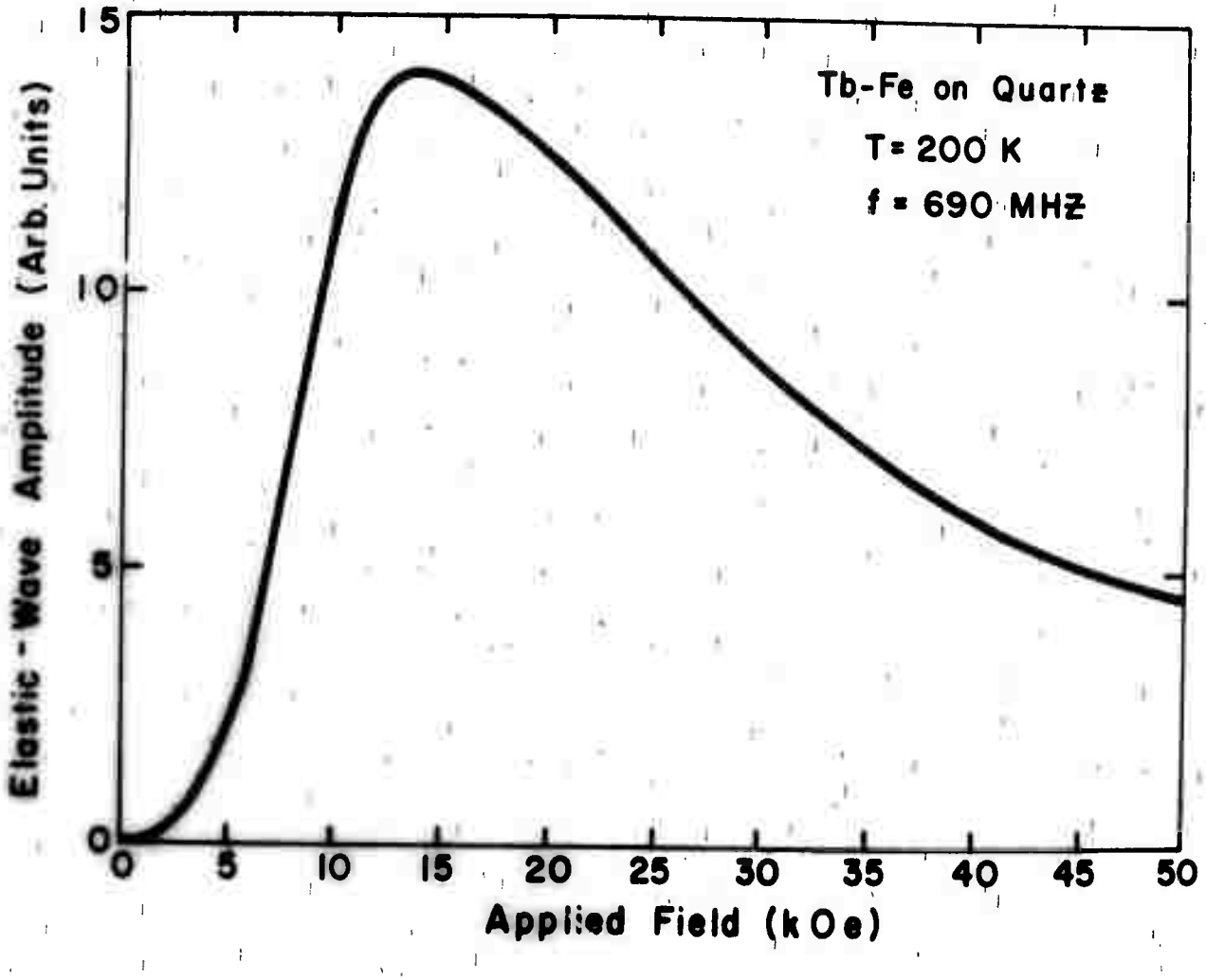

Fig. 12 Elastic-wave generation in a terbium-iron polycrystalline thin film as a function of applied magnetic field. The field is perpendicular to the plane of the film; the temperature is 200 K.

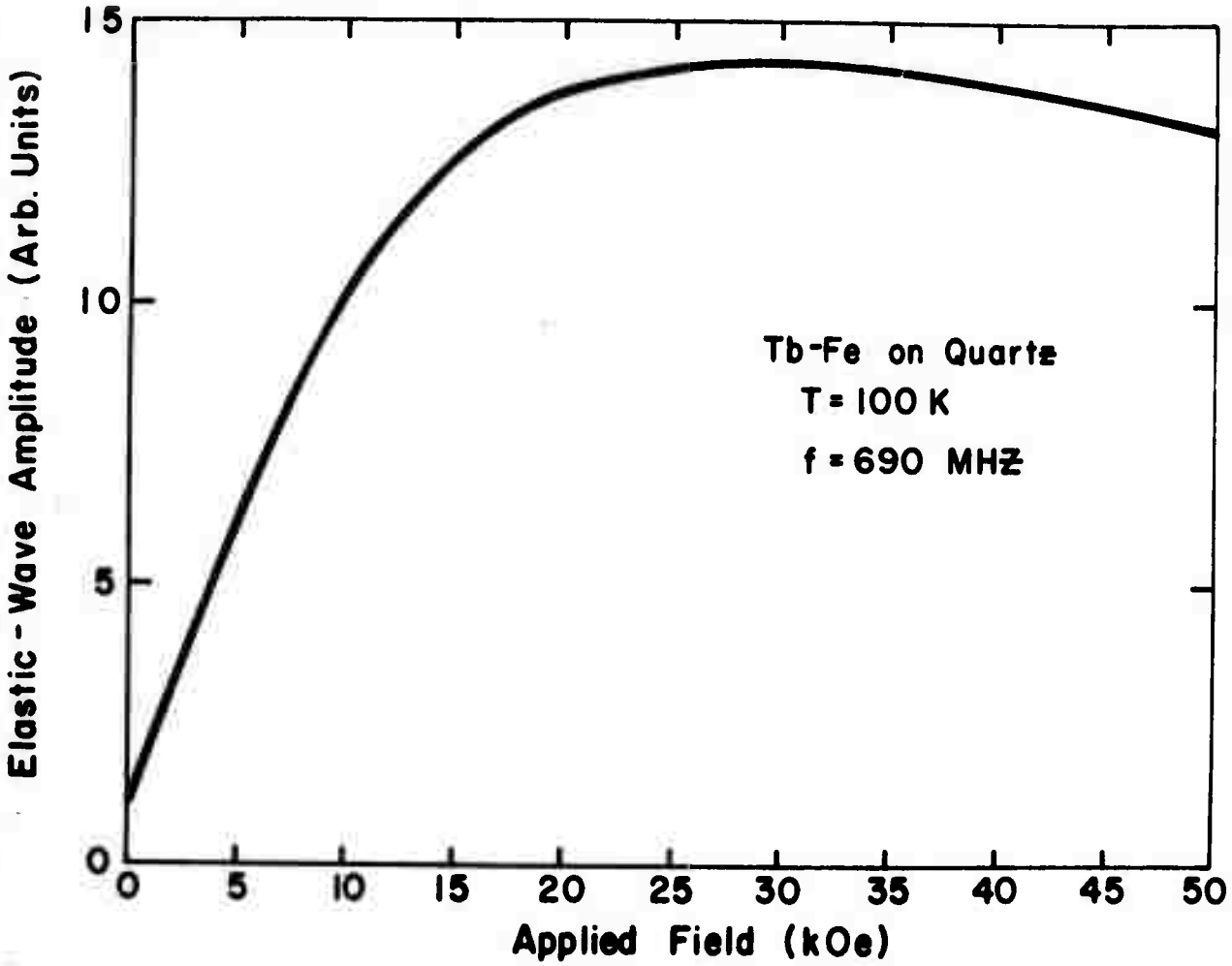

Fig. 13 Elastic-wave generation in a terbium-iron polycrystalline film as a function of applied magnetic field. The field is perpendicular to the plane of the film; the temperature is 100 K.

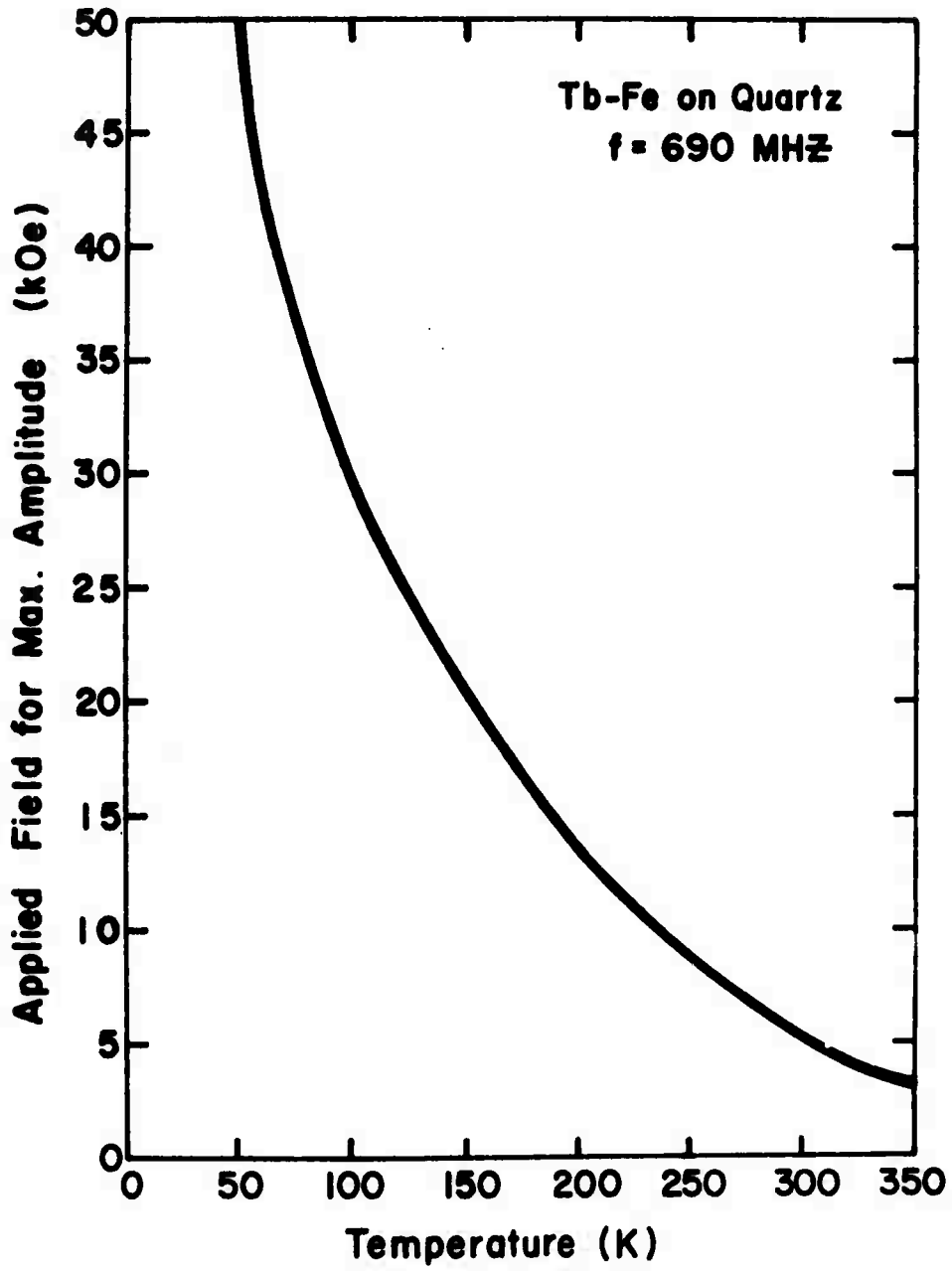

Fig. 14 Temperature dependence of the applied magnetic field at which elastic-wave generation is maximized in a terbium-iron polycrystalline thin film.

result of a simple uniform-precession ferrimagnetic resonance, involving only the terbium ions in the terbium-iron compound. The broadening which occurs at low temperature is undoubtedly the result of the magnetocrystalline anisotropy, which increases strongly at low temperatures, leading to a broadening in the polycrystalline films employed for this work, rather than to a frequency shift, which might be expected in the case of a single-crystal specimen.

The maximum intensity of the magnetostrictively generated shear elastic waves was also a function of temperature. The temperature dependence of the maximum intensity at a frequency of 690 MHz is shown in Fig. 15. It can be seen in this figure that the maximum intensity (that is, the maximum intensity vs. field strength) reaches its maximum value at a temperature of approximately 200K, decreasing by approximately 17 dB at a temperature of 300K. This variation with temperature is not understood at this time, although it might reasonably be expected that the elastic-wave intensity at this frequency would increase as the temperature is lowered from room temperature because of the temperature dependence of attenuation within the substrate and within the film itself. What is particularly not understood, however, is the decrease in the maximum intensity at temperatures below 200K, although this decrease is probably associated with the broadening of the resonant behavior at low temperatures.

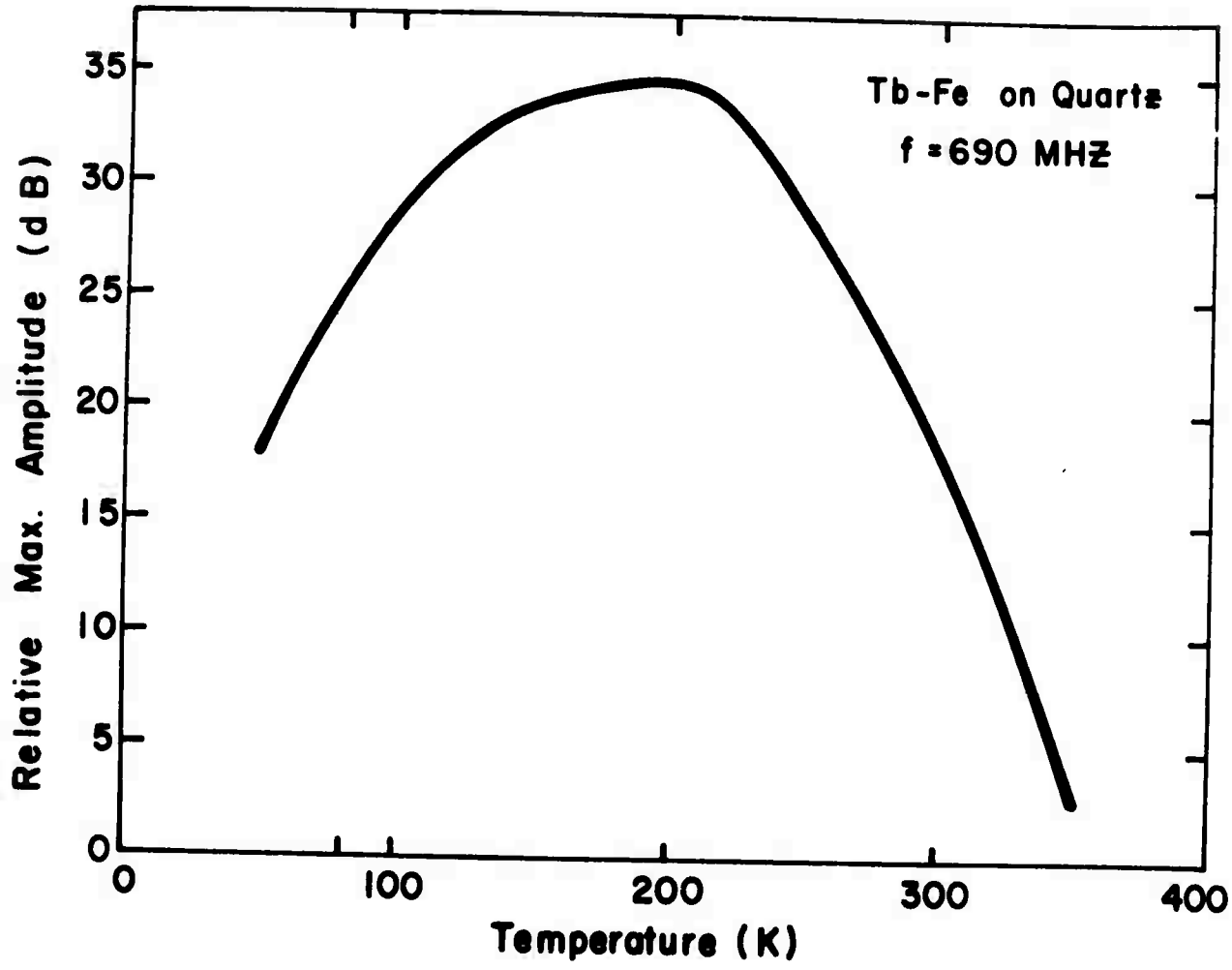

Fig. 15 Temperature dependence of elastic-wave generation in a terbium-iron polycrystalline thin film at the value of the applied field which maximizes the elastic-wave amplitude (See Fig. 14).

Although it has not yet been possible to determine the absolute efficiency of elastic-wave generation in terbium-iron films, a comparison has been made with piezoelectric generation in the quartz substrates on which the films were deposited. This comparison gives only a qualitative idea of the relative efficiency of generation, since the piezoelectrically generated waves in the X-cut quartz substrates were longitudinally polarized, whereas the magnetostrictively generated waves were transversely polarized. In this comparison, the same stripline resonant cavity was employed for both types of generation, with the substrate rod placed in the position within the cavity which optimized each type of elastic-wave generation. At a temperature of 200K, at which the magnetostrictive generation was most efficient, the intensity of the waves generated magnetostrictively was greater than that of the waves generated piezoelectrically, although of the same order of magnitude. In view of the unknown composition of the sample films used in this work, no attempt has yet been made to make a more accurate determination of the efficiency of generation.

Future work on the magnetostrictive generation of elastic waves in films of terbium-iron compounds and of other rare-earth-iron compounds will include an analysis of the chemical composition of the films in an effort to determine whether the evaporation process changes the composition from that of bulk material. A full

study of the effect of film thickness will also be carried out. It is believed that an optimum thickness will be found for each frequency of operation.

In summary, it has been shown that the large magnetostriction of terbium-iron compounds can be utilized for the generation of elastic waves at temperatures from 4.2K to 350K (substantially above normal ambient temperatures). Although not all the features of this magnetostrictive generation are well understood, reasonable agreement with the expected behavior was found at the higher temperatures within this range. A more systematic investigation of the generation process, with better control of film preparation and better knowledge of film concentration should permit the optimization of the generation process and the ultimate realization of the potential of the rare-earth-iron compounds as high-efficiency ultrasonic transducers.

3. Elastic-Wave Generation in Pure Rare-Earth Thin Films

In addition to the work on elastic-wave generation in thin films of terbium-iron compounds described in Section III.2, further work has been carried out on films prepared from the pure rare earths, dysprosium and terbium. Preliminary results on these and other materials have been reported previously[1,6]. The most significant results which can be reported here concern the relative

efficiency of elastic-wave generation in dysprosium films compared to piezoelectric generation in the quartz substrate upon which the dysprosium films were deposited. At all temperatures below the Curie temperature (T_C = 85K), the efficiency of elastic-wave generation in dysprosium was approximately 20 dB greater than that for piezoelectric generation in quartz at a frequency of 690 MHz. For terbium films, the most significant result is the occurrence of elastic-wave generation at temperatures above the Néel temperature (T_N = 229K). This represents the first observation of elastic-wave generation in a magnetostrictive thin film at frequencies above 100 MHz in the paramagnetic phase.

Although a more complete description of the results obtained with pure rare-earth films is in preparation, these results are summarized briefly here. The experimental arrangement was identical with that employed for the study of films of terbium-iron compounds described in Section III.2 of this report. Again, elastic-wave generation was obtained only with the applied dc magnetic field perpendicular to the plane of the film, and only transversely polarized elastic waves were generated.

Typical results are shown in Figs. 16 and 17, in which the magnetic-field dependence of elastic-wave generation is shown. In Fig. 16, the field dependence of the magnetostrictive generation of elastic waves in thin films of dysprosium is illustrated at a

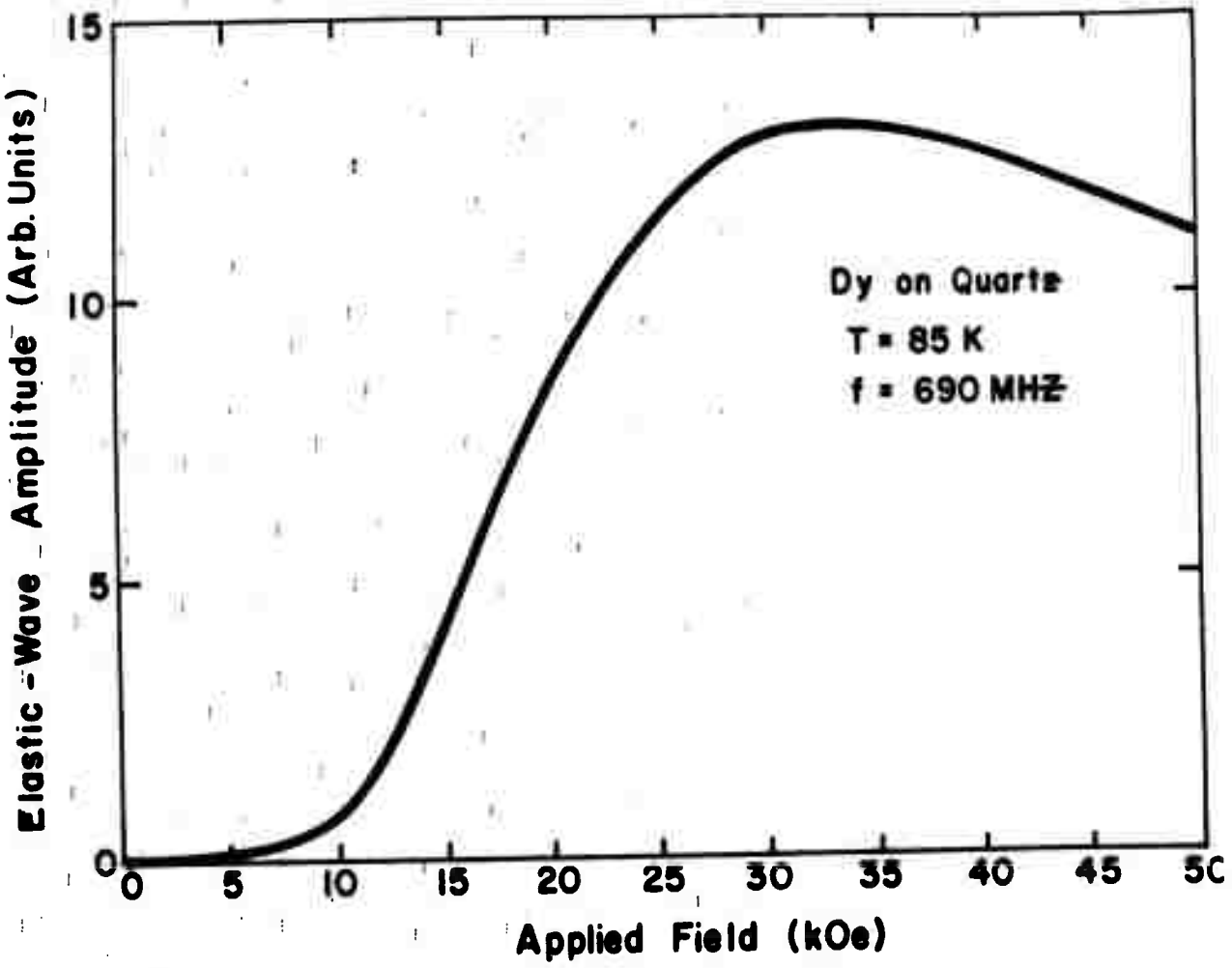

Fig. 16 Elastic-wave generation in a dysprosium polycrystalline thin film as a function of applied magnetic field. The field is perpendicular to the plane of the film; the temperature is 85 K.

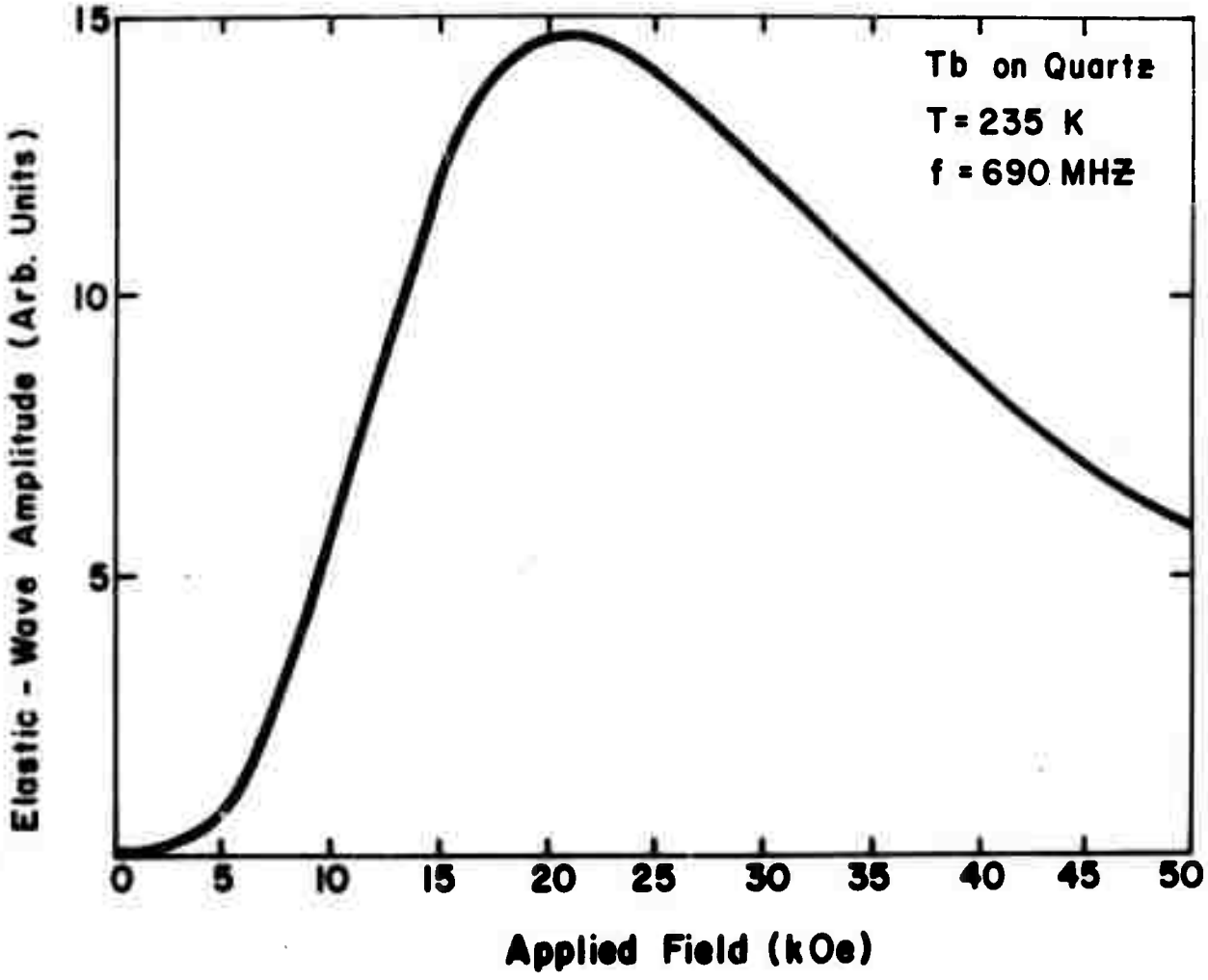

Fig. 17 Elastic-wave generation is a terbium polycrystalline film as a function of applied magnetic field. The field is perpendicular to the plane of the film; the temperature is 235 K.

temperature of 85K. It can be seen that there is a broad resonance, much the same as that observed in the case of the terbium-iron films. A similar result is shown for the case of terbium in Fig. 17, at a temperature of 235K (above T_N). The principal difference between the results obtained for these pure rare-earth films and those obtained for the terbium-iron films is the fact that the efficiency of ultrasonic generation in the pure rare-earth films increases monotonically as the temperature is lowered, in contrast to the situation in the terbium-iron films, where the efficiency decreases at temperatures below approximately 200K. Of course, in the case of the pure rare-earth films, there is no observable elastic-wave generation at room temperature, in contrast to the substantial elastic-wave generation observed at temperatures as high as 350K in the case of the terbium-iron films. Nevertheless, the efficiency of elastic-wave generation at low temperatures in films prepared from pure dysprosium is much greater than that which has been observed at any temperature in the case of the terbium-iron films.

Future work on films prepared from the pure rare earths will include studies on elastic-wave generation in thin films of the elements gadolinium, holmium, and erbium, in addition to further studies on dysprosium and terbium films. Elastic-wave transducers consisting of single-crystal disks of all of these pure rare earths

will also be investigated. It is believed that extremely high efficiencies can be ultimately obtained if ferromagnetic resonances can be excited in such single-crystal transducers. Preliminary work on single-crystal transducers of terbium and gadolinium has already been carried out[1], but the difficulty of forming a good acoustic bond between a highly magnetostrictive material and a substrate has made progress in this area slow. Elastic-wave generation in bulk single-crystal specimens of the pure rare earths will also be studied at frequencies low enough that the intrinsic attenuation of the bulk material does not preclude the observation of ultrasonic echoes. Preliminary work has shown the feasibility of these studies, but no systematic research has yet been carried out using bulk single-crystal material.

Although the investigation of elastic-wave generation in the pure rare earths cannot lead to the development of high-efficiency transducers for operation at room temperature and above, because of the low magnetic-ordering temperatures of the pure rare earths, it is expected that such studies, on materials whose properties are well documented and whose behavior is reasonably well understood in most respects will lead to an understanding of elastic-wave generation in rare-earth materials which will help in the exploitation of the rare-earth-iron compounds as high-efficiency, high-temperature transducers.

IV. THEORY OF MAGNETOELASTIC INTERACTIONS IN RARE-EARTH MATERIALS

In the annual report covering the research carried out during the first year of this program[1], a theoretical treatment of dynamical magnetoelastic interactions in rare-earth materials was described. The principal feature of this treatment was the development of coupled equations of motion for the dynamical variables of the system, including, in addition to the usual elastic-wave-amplitude variables and the magnetic-moment variables, equations of motion for the higher-order magnetic variables which are needed for a complete description of a system of magnetic moments. In most previous treatments of the magnetic and magnetoelastic properties of rare-earth materials, these higher-order variables have been either ignored completely or treated by means of approximations of questionable validity. It is expected that the present treatment will lead to more accurate predictions of the characteristics of such phenomena as magnetostrictive elastic-wave generation than have been possible using previous theoretical treatments[8-10].

Although there are many problems of interest which can ultimately be solved through the use of the theoretical treatment presented here, only two closely related examples are worked out in detail here: the linear and circular magnetoacoustic birefringence for shear elastic waves at low frequency (MHz range) propa-

gating along the hexagonal axis in an anisotropic system such as terbium or dysprosium. The principal reason for the choice of these examples lies in the simplicity which arises from the consideration of only low-frequency elastic waves, for which the interaction with spin waves of finite wavelength is small. Furthermore, because of the restriction to low frequencies (compared to normal spin-wave frequencies), problems such as spin-wave relaxation can be avoided. The two examples presented in this section are also closely related to the experimental work described in Section II.1, but the theoretical results derived here are somewhat different from those used in the interpretation of the experimental results in Section II.1. Actually, the results obtained by means of the present treatment are qualitatively quite similar to those given in Section II.1, but they permit a somewhat different interpretation of the experimental results with respect to the determination of the fundamental shear magnetoelastic coupling constant.

1. Equations of Motion for Dynamic Magnetoelastic Effects in the Rare Earths

In the derivation of coupled equations of motion for the magnetic and elastic variables of a magnetostrictive system, it is convenient to consider the elastic waves classically, developing

classical wave equations for the elastic-wave amplitudes in the long-wavelength continuum limit. These wave equations contain terms which couple the elastic waves to the magnetic ions of the system and which are proportional to the expectation values of certain quantum-mechanical angular-momentum operators. For the angular-momentum operators which describe the dynamic state of the magnetic ions, it is most convenient to develop equations of motion of the Heisenberg type. Such equations will also, in the present case, contain terms proportional to the elastic-wave variables. The complete solution of the coupled set of equations of motion will, in principle, permit the description of a great variety of dynamic magnetic and magnetoelastic phenomena. Unfortunately, the total number of equations of motion required to describe the magnetic system completely, even using the molecular-field approximation and assuming uniform-precession behavior for the angular-momentum variables, can be very large for systems for which the ionic angular momentum is large. Such is the case for all the heavy rare earths. In order to find a solution to the equations of motion without the use of numerical computation, it is necessary to make certain approximations which may in some cases affect the validity of the solutions to the equations of motion. Fortunately, for the phenomena of magnetoacoustic birefringence, the necessary approximations for the simpler rare earths, such as

terbium and dysprosium, are not of such a nature as to impair the validity of the results.

In what follows, the molecular-field approximation is employed to account for exchange effects. Although this approximation is not valid for the description of all phenomena in magnetically ordered materials, its range of validity covers so many aspects of the behavior of many types of magnetically ordered solids, particularly at high temperatures, that its simplicity makes it a very widely used approximation. In the present problem, attention is given primarily to such materials as terbium in the paramagnetic phase just above the Néel temperature and in the ferromagnetic phase below the Curie temperature or between T_C and T_N, but in the presence of an applied magnetic field sufficient to induce the transition from the helimagnetic to the ferromagnetic phase. In this manner, the exact consideration of the helimagnetic phase is avoided for the present treatment, and the use of a simple molecular-field constant is justified. No important restriction is involved in the case of terbium, for which the critical field is less than 1 kOe, but a more careful consideration of the helimagnetic region would be necessary in order to treat the case of dysprosium properly at all temperatures and at all values of the applied magnetic field.

The Hamiltonian for the coupled magnetoelastic system is composed of three parts:

$$\mathcal{H} = \mathcal{H}_m + \mathcal{H}_{me} + \mathcal{H}_e \ . \tag{1}$$

The purely magnetic part of the Hamiltonian, $\mathcal{H}_m$, is made up of the Zeeman energy of the magnetic moments of the individual rare-earth ions in a magnetic field consisting of the resultant of the applied field, the demagnetizing field, and the molecular field, plus the magnetocrystalline energy due to crystalline electric fields. In the present treatment, a uniaxial crystal-field term is included, but the other possible terms, such as the sixth-rank basal-plane anisotropy, are omitted for simplicity. This neglect is probably not important at temperatures not far below the Curie temperature. Thus, the magnetic part of the Hamiltonian may be expressed as:

$$\mathcal{H}_m = g\mu_B[\vec{H}-N\vec{M}+\Gamma\vec{M}] \cdot \sum_i \vec{J}_i + P_2 \sum_i J_{3i} \ . \tag{2}$$

In Eq. (2), g is the spectroscopic splitting factor for the rare-earth ions, μ_B is the Bohr magneton, $\vec{H}$ is the applied magnetic field, N is the demagnetizing factor, assumed isotropic, as in the case of a spherical sample, $\vec{M}$ is the magnetization of the sample, parallel to $\vec{H}$, $\vec{J}_i$ is the angular momentum operator for the i^{th} ion, and J_{3i} is one of the five independent, Hermitian, second-rank angular-momentum tensor operators defined below, for the i^{th} ion.

The definition of the second-rank operators appearing in the crystal-field term of Eq. (2) is necessary at this point, since these operators will play an important role in the remainder of this work. These operators are merely linear combinations of the five second-rank irreducible-tensor angular-momentum operators commonly used in many angular-momentum problems[37], and they are defined as follows:

$$J_{12} = J_x^2 - J_y^2 \qquad J_4 = J_yJ_z + J_zJ_y$$

$$J_3 = 3J_z^2 - J(J+1) \qquad J_5 = J_xJ_z + J_zJ_x$$

$$J_6 = J_xJ_y + J_yJ_x \tag{3}$$

The elastic part of the Hamiltonian, $\mathcal{H}_e$, is just the classical continuum Hamiltonian, expressed in terms of the particle-displacement amplitudes, the elastic strains (which are expressed as derivatives of the displacement amplitudes), the elastic constants of the material, and the density. This part of the Hamiltonian can be expressed as

$$\mathcal{H}_e = \int_V \left[\frac{1}{2} \sum_{i,j} c_{ij} e_i e_j + \frac{1}{2} \rho \left(\frac{\partial \vec{u}}{\partial t} \right)^2 \right] dV \ . \tag{4}$$

In Eq. (4), $\vec{u}$ is the particle-displacement amplitude, and the quantities e_i are the conventionally defined engineering strains, expressible as derivatives of the displacement amplitudes. The

integration covers the entire volume of the sample, and it is assumed that the displacement amplitude and the associated strain components vary both in time and space in a wavelike fashion.

The magnetoelastic part of the Hamiltonian couples the elastic strain components to the second-rank angular-momentum operators defined in Eqs. (3), utilizing four coupling constants, B_1-B_4. This form for the magnetoelastic Hamiltonian is based upon the assumption that the total magnetoelastic interaction is the result of strain modulation of the magnetocrystalline energy, and it ignores the possibility of strain modulation of the exchange energy. Actually, there is some evidence[38,39] for the existence of an appreciable exchange magnetostriction, but, for simplicity, only the crystal-field single-ion magnetostriction is considered here. The magnetoelastic Hamiltonian is written as follows:

$$\mathcal{H}_{me} = B_1[(e_1-e_2)\sum_i J_{12i} + e_6\sum_i J_{6i}] + B_4[e_4\sum_i J_{4i} + e_5\sum_i J_{5i}] + [B_2(e_1+e_2) + B_3e_3]\sum_i J_{3i} \quad . \tag{5}$$

In the development of the equations of motion, it is assumed that the time and space variation of the elastic variables is plane-wave-like, and that the variation of the magnetic variables is also plane-wave-like, with the same frequency and wave vector. For the purpose of the present problem, it is assumed that shear

elastic waves are propagated along the z-axis (the hexagonal crystalline axis), and that they are accompanied by a wavelike perturbation of the eight independent first- and second-rank angular-momentum operators, induced by the magnetoelastic coupling. Thus, only the elastic strains e_4 and e_5 are considered, and the associated displacement amplitudes are denoted, respectively, v and u.

If the continuum Hamiltonian classical mechanics described by Goldstein[40] is employed for the development of the elastic equations of motion, the following equations result:

$$\rho \frac{\partial^2 u}{\partial t^2} = c_{44} \frac{\partial^2 u}{\partial z^2} + B_4 N \frac{\partial J_5}{\partial z} \tag{6}$$

$$\rho \frac{\partial^2 v}{\partial t^2} = c_{44} \frac{\partial^2 v}{\partial z^2} + B_4 N \frac{\partial J_4}{\partial z} \tag{7}$$

In Eqs. (6) and (7), the quantity N is the number of magnetic ions per unit volume, and the angular-momentum operators, both here and in the subsequent equations of motion are understood to be the expectation values of these quantities. These equations of motion for the elastic-wave amplitudes, without the magnetoelastic coupling, would be the usual equations for shear-wave propagation along a hexagonal axis, yielding two degenerate shear waves. In order to solve the equations, it is necessary to examine the equations of motion for the angular-momentum variables.

The equations of motion for the angular-momentum operators are obtained by evaluating the time derivatives of the eight independent first- and second-rank tensor operators according to the Heisenberg method:

$$\dot{F} = (i/\hbar)\ [\mathcal{H},F]\ , \tag{8}$$

where F is any Hermitian operator and $\mathcal{H}$ is the Hamiltonian of the system of interest. In Eq. (8), it is understood that the expectation value of both sides of the equation is implied.

Before the actual evaluation of the equations of motion, it is necessary to decide upon the particular problem whose solution is desired. Two problems of interest are to be presented here: the circular birefringence of the shear elastic waves propagating along the hexagonal axis, with the applied magnetic field and the magnetization of the sample along this axis, and the linear birefringence, similar to that reported in Section II.1, in which the applied field and the magnetization are both directed in the plane perpendicular to the hexagonal axis, the so-called basal plane. In the case of the circular birefringence, the magnetization must develop an appreciable component along the hexagonal axis, but for both terbium and dysprosium, the uniaxial anisotropy, represented by the crystal-field constant P_2 in Eq. (2), confines the magnetization to the basal plane below the Néel temperature.

Consequently, only a small component of magnetizations can be induced by an applied field along the hexagonal axis, and there will be, in general, at temperatures below T_N, a large component of spontaneous magnetization lying in the basal plane. Consequently, in the treatment of circular magnetoacoustic birefringence given here, it will be assumed that the uniaxial anisotropy term, characterized by P_2, is opposite to that found in terbium or dysprosium, giving rise to an easy axis of magnetization along the hexagonal direction. For the case of the linear magnetoacoustic birefringence, however, the same type of easy-plane anisotropy found in terbium and dysprosium will be employed.

2. Equations of Motion for Circular Magnetoacoustic Birefringence

In this case, as stated above, in order to avoid the complications which would arise from treatment of a system with a preferred direction of magnetization different from the intended direction of the applied magnetic field, the constant, P_2, of Eq. (2) is assumed to be negative. In this case, the preferred direction for the spontaneous magnetization will lie along the z-axis, and it is unnecessary in the following analysis to change the method of treatment in going from the paramagnetic to the ordered magnetic phase.

The equations of motion for a typical rare earth such as terbium, with J = 6, or dysprosium, with J = 15/2, would require a total of 4J(J+1) equations for a complete description of all the dynamic properties of the system. In the following development of the equations of motion, however, in the interest of simplicity, only the eight equations of motion for the first- and second-rank angular-momentum operators are developed, since they are sufficient for the explanation of the observed phenomena. It is felt that the neglect of the higher order equations of motion will result in only a small degree of error, and it should be pointed out that the inclusion of even the second-rank operators in the present theory represents a better approximation to the complete system of equations than that used in previous treatments of this and similar problems[8-10,14].

The equations of motion for the angular-momentum variables are the following:

$$\dot{J}_x = \omega_y J_z - \omega_z J_y + 3P_2 J_4 + B_4(J_{12}+J_3)e_4 - B_4 J_6 e_5 \tag{9}$$

$$\dot{J}_y = \omega_z J_x - \omega_x J_z - 3P_2 J_5 + B_4 J_6 e_4 - B_4(J_3-J_{12})e_5 \tag{10}$$

$$\dot{J}_z = \omega_x J_y - \omega_y J_x - B_4 J_5 e_4 - B_4 J_4 e_5 \tag{11}$$

$$\dot{J}_{12} = \omega_x J_4 + \omega_y J_5 - 2\omega_z J_6 - B_4 J_x e_4 - B_4 J_y e_5 \tag{12}$$

$$\dot{J}_6 = -\omega_x J_5 + \omega_y J_4 + 2\omega_z J_{12} - B_4 J_y e_4 + B_4 J_x e_5 \tag{13}$$

$$\dot{J}_3 = 3\omega_x J_4 - 3\omega_y J_5 - 3B_4 J_x e_4 - 3B_4 J_y e_5 \tag{14}$$

$$\dot{J}_4 = -\omega_x(J_{12}+J_3) - \omega_y J_6 + \omega_z J_5 - 3P_2 J_x - B_4 J_z e_5 \tag{15}$$

$$\dot{J}_5 = \omega_x J_6 - \omega_y(J_{12}-J_3) - \omega_z J_4 + 3P_2 J_5 + B_4 J_z e_4 \tag{16}$$

The various frequencies, ω_x, ω_y, and ω_z, appearing in Eqs. (9)-(16) are defined as follows:

$$\omega_x = g\mu_B[H_x + (\Gamma-N)M_x] \tag{17}$$

$$\omega_y = g\mu_B[H_y + (\Gamma-N)M_y] \tag{18}$$

$$\omega_z = g\mu_B[H_z + (\Gamma-N)M_z] \tag{19}$$

In order to obtain the desired solution of the equations of motion, leading to the circular magnetoacoustic birefringence, it is necessary to specify that the applied magnetic field lies in the z-direction, and that the equilibrium magnetization also lies in this direction. In this situation, the angular-momentum operators J_z and J_3 will have non-zero equilibrium values which can be expressed in terms of the theory of equilibrium properties of magnetic materials of Callen and Callen[41]:

$$J_z^{\,o} = -J\sigma \tag{20}$$

$$J_3^{\,o} = 2J(J-1/2)\,\hat{I}_{5/2}[L^{-1}(\sigma)] \tag{21}$$

In Eqs. (20) and (21), the quantity σ is the reduced magnetization, M_z/M_o, where M_o is the zero-temperature saturation magnetization, the function $\hat{I}_{5/2}$ is the reduced modified Bessel function defined by Callen and Callen[41], and the function L^{-1} is the inverse Langevin function. Thus, if the reduced magnetization can be determined, these equilibrium values of the angular-momentum operators may be evaluated when needed.

If the elastic-wave variables, e_4 and e_5, are regarded as classical parameters, and the angular-momentum variables are regarded as dynamical variables, the equations of motion for the angular-momentum variables, Eqs. (9)-(16), can, in principle, be solved for the values of all the angular-momentum variables as functions of the elastic strains. These equations are, however, nonlinear, in that they contain products of dynamical variables. They can, nevertheless, be solved in a linear approximation which is appropriate for the present problem. In this linearization of the equations, all products of two or more dynamical variables are neglected on the grounds that such terms will be small compared to terms which are of first order in these variables.

The linearized form of the equations appropriate for the problem of circular birefringence is then the following:

$$\dot{J}_x = -\omega_1 J_y + 3P_2 J_4 + B_4 J_3^{\circ} e_4 \tag{22}$$

$$\dot{J}_y = \omega_1 J_x - 3P_2 J_5 - B_4 J_3^{\circ} e_5 \tag{23}$$

$$\dot{J}_4 = \omega_2 J_x + \omega_3 J_5 - B_4 J_z^{\circ} e_5 \tag{24}$$

$$\dot{J}_5 = -\omega_2 J_y - \omega_3 J_4 + B_4 J_z^{\circ} e_4 \tag{25}$$

$$\dot{J}_{12} = -2\omega_3 J_6 \tag{26}$$

$$\dot{J}_6 = 2\omega_3 J_{12} \tag{27}$$

$$\dot{J}_z = \dot{J}_3 = 0 \tag{28}$$

In the above linearized form for the equations of motion, the frequencies ω_1, ω_2, and ω_3 are defined as

$$\omega_1 = g\mu_B H, \quad \omega_2 = \omega_o J_3^{\circ} - 3P_2, \quad \omega_3 = \omega_1 - \omega_o J_z^{\circ}, \quad \omega_o = g\mu_B \Gamma M_o \tag{29}$$

At this point, it must be remembered that only the solutions for the operators J_4 and J_5 as functions of e_4 and e_5 are needed for the solution of the wave equations, Eqs. (6) and (7) in this birefringence problem. Thus, only the coupled equations for J_x, J_y, J_4, and J_5, Eqs. (22)-(25) need be solved. Under the assumption of a complex exponential time dependence for these operators at a frequency ω, with the same time dependence for the strain variables, e_4 and e_5, Eqs. (22)-(25) can be solved to give the following expressions for J_4 and J_5:

$$J_4 = \alpha(M,H) e_4 + i\omega\beta(M,H) e_5 \tag{30}$$

$$J_5 = \alpha(M,H) e_5 - i\omega\beta(M,H) e_4 \tag{31}$$

In Eqs. (30) and (31), the functions α and β are derived in the limit in which the angular frequency, ω, is small compared to all the frequencies defined in Eq. (29). In this limit, which implies that the frequency of the elastic waves is in the range of several MHz (possibly up to several hundreds of MHz), the functions α and β take the following form:

$$\alpha(M,H) = B_4[J_z^{\circ}(3P_2\omega_1\omega_2+\omega_1^2\omega_3) - J_3^{\circ}(3P_2\omega_2^2 + \omega_1\omega_2\omega_3)]/D \quad (32)$$

$$\beta(M,H) = B_4[J_z^{\circ}(\omega_1^2-3P_2\omega_2) - J_3^{\circ}(\omega_1\omega_2 - \omega_2\omega_3)]/D \quad (33)$$

$$D(M,H) = [\omega_1\omega_3 + 3P_2\omega_2]^2 \quad (34)$$

All the quantities appearing in Eqs. (32)-(34) have been previously defined and can be expressed in terms of the static magnetic properties of the material. Before a consideration, however, of such characteristics of these functions as their dependence on temperature or applied field, it is necessary to consider the way in which the results given in Eqs. (30) and (31) lead to circular magnetoacoustic birefringence.

The wave equations for the two elastic-wave amplitudes, Eqs. (6) and (7), become, upon substitution of the expressions given in Eqs. (30) and (31) for J_4 and J_5,

$$\rho \frac{\partial^2 u}{\partial t^2} = c_{44} \frac{\partial^2 u}{\partial z^2} + B_4 N \left[\alpha \frac{\partial^2 u}{\partial z^2} + i\omega\beta \frac{\partial^2 v}{\partial z^2} \right] \tag{35}$$

$$\rho \frac{\partial^2 v}{\partial t^2} = c_{44} \frac{\partial^2 v}{\partial z^2} - B_4 N \left[\alpha \frac{\partial^2 v}{\partial z^2} - i\omega\beta \frac{\partial^2 u}{\partial z^2} \right] \tag{36}$$

From these equations, it can be seen that the magnetoelastic coupling provides a coupling of the two wave equations for the two normally independent components of the elastic-wave amplitude. That this coupling leads to circular birefringence can be easily seen by expressing the coupled equations in terms of the circularly polarized elastic-wave amplitudes,

$$u^+ = u + iv \qquad u^- = u - iv \tag{37}$$

With these definitions, the sum of Eqs. (35) and (36) becomes

$$\rho \frac{\partial^2 u^+}{\partial t^2} = c_{44}^+ \frac{\partial^2 u^+}{\partial z^2} \quad , \tag{38}$$

whereas the difference of the two coupled wave equations becomes

$$\rho \frac{\partial^2 u^-}{\partial t^2} = c_{44}^- \frac{\partial^2 u^-}{\partial z^2} \quad . \tag{39}$$

with the effective elastic constants for shear circularly polarized elastic waves, c_{44}^+ and c_{44}^-, given by the following:

$$c_{44}^+ = c_{44} + NB_4[\alpha+\omega\beta] \tag{40}$$

$$c_{44}^- = c_{44} + NB_4[\alpha-\omega\beta] \quad . \tag{41}$$

The phase velocities for the two independent circularly polarized shear waves are, as usual, given by $v_{\pm}^{2} = c_{44}^{\pm}/\rho$, so that, if the difference in velocities is defined as

$$\Delta v/v = (c_{44}^{+} - c_{44}^{-})/2c_{44} , \tag{42}$$

then the rotation of the plane of polarization of a linearly polarized shear wave propagating along the z-axis, per unit length of travel, can be written as

$$\phi/\ell = \frac{\omega}{v} (\Delta v/v) = \omega^{2} N B_{4} \beta(M,H)/\rho v^{3} \tag{43}$$

From Eq. (43), it can be seen that, subject to the approximations discussed above and within the low-frequency range for which the angular frequency of the elastic waves is small compared to any of the natural ferromagnetic-resonance frequencies of the material, the angular rotation per unit length is proportional to the square of the angular frequency, ω. The dependence of the specific rotation on temperature and applied magnetic field strength lies entirely in the function, $\beta(M,H)$, defined in Eq. (33). The qualitative nature of the field dependence of β can easily be seen. In the paramagnetic phase, both J_{z}^{o} and J_{3}^{o} are equal to zero in the absence of an applied field, and the denominator, D, approaches a constant value, $(3P_{2})^{4}$, as the field approaches zero. Therefore, as expected, there is no birefringence when the material is unmagnetized. At a given

temperature, in the paramagnetic phase, both J_z^o and J_3^o increase in magnitude with increasing field. The other quantities which serve to determine β also vary with field, but the variation of β with field, due to the variation of all its factors, may be somewhat complex, since the function depends upon the differences of several terms. It is undoubtedly true, however, that β increases in magnitude initially as the applied field increases. The initial slope and the behavior at high field values, however, will depend upon the initial magnetic susceptibility of the material and upon the way in which the magnetization approaches saturation at high field values. At temperatures in the magnetically ordered range, the behavior is more complicated: The initial birefringence will depend upon the remanent magnetization, which will, of course, depend upon the previous history of magnetization of the material. The field dependence of β will probably exhibit a rapid approach to a saturation value as the field is increased from zero, corresponding to the saturation of the magnetization as a small field is applied along an easy axis.

Since no experimental data have yet been obtained on circular magnetoacoustic birefringence in the research program described in this report, the exact behavior of the function $\beta(M,H)$ is not further explored at this time. A more complete treatment of both the circular and the linear magnetoacoustic birefringence in the rare earths is, however, in preparation.

3. Equations of Motion for Linear Magnetoacoustic Birefringence

The phenomenon of linear magnetoacoustic birefringence is of more interest for the present work than is the phenomenon of circular birefringence discussed in Section IV.2 above, since experimental data have been obtained for this effect. The theoretical treatment of linear birefringence is quite similar to that used for circular birefringence, although there are certain significant differences concerning the nature of the material in which the linear effect may be observed. The principal difference is the assumption that the equilibrium direction of the spontaneous magnetization is perpendicular to the direction of elastic-wave propagation. That is, for the present case, it is assumed that the basal plane, perpendicular to the hexagonal axis, is an easy plane of magnetization. Thus, the constant P_2 appearing in Eq. (2) is assumed to be positive, in contrast to the preceding case. This situation is applicable to rare earths such as terbium and dysprosium. It is further assumed that the applied field is directed along the magnetization, perpendicular to the direction of propagation. With these two assumptions, the treatment of the problem is identical to that employed in the case of the circular birefringence, except that in the present case it is necessary to compute the velocity when the field and magnetization are directed parallel to

and perpendicular to the elastic-wave polarization. The difference in the phase velocity obtained in the two cases then leads to the linear birefringence effect.

In the present case, the velocity of shear elastic waves propagating along the hexagonal axis, with the polarization vector directed along the x-axis, is calculated for the applied field and magnetization both parallel to and perpendicular to the polarization vector. For a material such as terbium or dysprosium, the basal-plane anisotropy, which becomes important at temperatures substantially below the magnetic ordering temperature, is neglected in the present analysis. This neglect of the basal-plane anisotropy is unimportant at temperatures in the paramagnetic range, and it probably will have no significant qualitative effect upon the results of the analysis at temperatures somewhat below the ordering temperature. For lower temperatures, when the field and magnetization are directed along the easy direction in the basal plane, the neglect of the basal-plane anisotropy is probably insignificant, but when the magnetization and field are directed along a non-equilibrium direction the basal-plane anisotropy should be considered in the analysis in order to obtain the correct equilibrium relationship between the applied field and the magnitude and direction of the magnetization. It should be pointed out that the experiment on birefringence described in Section II.1 was performed with the applied field at an angle of 15° from an easy direction.

Since only elastic waves polarized along the x-axis are considered in the present case, it is necessary to solve only the wave equation corresponding to this polarization, Eq. (6). In this equation, the only angular-momentum variable which appears is J_5, so that, following the analysis of Section IV.2, it is necessary to obtain J_5 as a function of e_5 and of the applied field, the magnetization, and the other quantities characterizing the magnetic material. The following result is obtained:

Field Parallel to Polarization:

$$J_5 = B_4 e_5 \frac{\left[\omega_1 J_z^{\,o} - \omega_4 (J_{12}^{\,o} + J_3^{\,o})\right]}{[\omega_1 \omega_3 + 3P_2 \omega_4]} \tag{44}$$

Field Perpendicular to Polarization:

$$J_5 = B_4 e_5 J_z^{\,o} / \omega_3 \tag{45}$$

In Eqs. (44) and (45), the quantities ω_1, ω_3, $J_z^{\,o}$, and $J_3^{\,o}$ have been previously defined in Eqs. (20), (21), and (29), and the quantities ω_4 and $J_{12}^{\,o}$ are defined as follows:

$$\omega_4 = \omega_o (J_3^{\,o} - J_{12}^{\,o}) \tag{46}$$

$$J_{12}^{\,o} = -\frac{3}{2} P_2 / \omega_3 \tag{47}$$

If the expressions given in Eqs. (44) and (45) are used to compute the difference in phase velocities for waves polarized parallel to and perpendicular to the applied field, and, from this difference in velocities, the phase-angle difference per unit length of travel for two perpendicularly polarized waves, the following results are obtained:

$$\Delta v/v = NB_4^2\left(\frac{\left[\omega_1 J_z^{\circ} - \omega_4 (J_{12}^{\circ} + J_3^{\circ})\right]}{[\omega_1\omega_3 + 3P_2\omega_4]} - \frac{J_z^{\circ}}{\omega_3}\right)/\rho v^2 \qquad (48)$$

$$\phi/\ell = \frac{\omega}{v}(\Delta v/v) \qquad (49)$$

It should be observed in Eq. (48) that there is no difference in velocity in an unmagnetized specimen, for which $J_z^{\circ} = J_3^{\circ} = J_{12}^{\circ} = 0$. Thus, in an unmagnetized specimen there will be no observable birefringence. As a field is applied, however, the birefringence develops, increasing as the induced magnetization increases. The dominant field-dependent term in Eq. (48) is probably the term $\omega_4(J_{12}^{\circ} + J_3^{\circ})$, which, in the paramagnetic phase, should increase as the fourth power of the applied field. This rapid rate of increase is, however, counteracted by the denominator of the same term, which also increases with increasing field. The exact numerical behavior of the expression given in Eq. (48) has not yet been calculated.

The field dependence of the linear magnetoacoustic birefringence, calculated according to the theory presented here, exhibits a strikingly different behavior from that described in Section II.1, based upon earlier theories[8-10]. It appears, however, that there is no really fundamental difference between the two theories. The apparent difference in the results arises from the assumption in the results quoted in Eq. (5) of Section II.1 that the magnetoelastic coupling can be expressed in terms of a field-independent coupling constant, b. In fact, the quantity, b, which is alternatively expressed as $b = c_{44}\lambda^{\epsilon}$, where λ^{ϵ} is the shear magnetostriction, is dependent upon the magnetization and, hence, upon the applied field. According to the theory of the equilibrium magnetic and magnetoelastic properties of the rare earths due to Callen and Callen[41], the quantity λ^{ϵ} should vary with field in the same manner as the quantity J_3^{o}, approximately as M^2 (or H^2 in the paramagnetic phase). With this interpretation of the magnetoelastic coupling constant, b, it can be seen that the predicted birefringence obtained from Eq. (5) of Section II.1 will exhibit approximately the same field dependence as that predicted in Eqs. (48) and (49) of the present treatment. It might be asked how the experimental results depicted in Fig. 4 give such good agreement with the field dependence predicted by Eq. (5) of Section II.1 under the assumption that the quantity, b, is field independent.

The apparent answer is that the agreement is coincidental. The curves of Fig. 4 were obtained under the assumption that the phase shift per unit length is the decreasing function of the applied field predicted by Eq. (5), Section II.1. Thus, the data used in plotting the data points in this figure were plotted under the assumption that the birefringence is, in fact, a decreasing function of the applied field. Under the opposite assumption, namely that the birefringence increases with applied field, starting from zero at zero applied field, an entirely different set of curves would have been obtained.

It is interesting to note that the data shown in Fig. 1 provide a verification of the present theoretical treatment and its finding that the birefringence should increase with increasing field. In this figure, which represents the dependence of the shear elastic-wave velocity upon the direction of the applied magnetic field, at a temperature of 240K and a frequency of 30 MHz, in an applied magnetic field of magnitude 10 kOe, the variation of the velocity is such that the velocity difference between the parallel-field and perpendicular-field cases is approximately $\Delta v/v = 1.4 \times 10^{-3}$. This velocity difference leads to a phase difference per unit length, $\phi/\ell = 1.55\ cm^{-1}$. This value for the phase difference exceeds all the values shown in Fig. 4, particularly those obtained at a temperature of 230K, even though the result obtained using the direct

measurement of birefringence given in Fig. 1 applies to a temperature of 240K, for which the birefringence should be smaller than at 230K.

It might be argued that the birefringence results obtained by Guermeur et al.[42] at a frequency of 9.3 GHz in yttrium iron garnet (YIG) support the earlier theories[8-10]. However, their work was done at a temperature of 4.2K, at which the YIG is completely saturated magnetically, so that all magnetization-dependent quantities, such as the magnetostriction, are field-independent. In this case, the previous theories agree in most respects with the present treatment. The same remarks apply to the agreement of the results of Moran and Lüthi[14] on magnetoacoustic birefringence in magnetite at temperatures from room temperature down to 125K. The Curie temperature of magnetite is approximately 860K, and the magnetization (and all magnetization-dependent quantities) is nearly saturated in the temperature range of this experiment. Thus, the quantity b in both of these experiments[14,42] can be properly regarded as a field-independent constant.

In view of the discrepancy between the present theoretical treatment and the experimental results of Section II.1 on linear magnetoacoustic birefringence, further work on both the theory and the interpretation of the experimental data is in progress. It is hoped that the present theory, with its ability to treat

magnetocrystalline anistropy in a consistent manner in all magnetic phases[1] will ultimately lead to good agreement with all pertinent experimental results. It is further expected that the theory presented here will soon be applied to the problem of magnetostrictive ultrasonic generation, which is somewhat more difficult than the birefringence examples presented here.

V. MATERIALS PREPARATION AND HOLOGRAPHIC MEASUREMENT OF MAGNETOSTRICTION

This section of this report describes two projects which have only recently been undertaken and for which results are not yet sufficient to warrant an extended description. Because of the importance of the terbium-iron compounds discussed in Section III, a project has been started to attempt the preparation of compounds of this type, consisting of the various rare earths and iron. The first specimens of terbium-iron compounds have been obtained, but their properties have not yet been determined. Rapid progress is expected, however, during the second six-month period covered by the present research contract. A second project has also been initiated to permit the study of magnetostriction in rare-earth elements, alloys, and compounds by means of holographic interferometry. The advantages of this method over the more conventional strain-gauge or capacitative methods include the ability to determine all modes of magnetostrictive strain simultaneously, and the ability to measure strain in small, irregularly shaped specimens. Furthermore, inhomogeneous strains, such as torsional strain, can be measured by this technique. Only preliminary results have yet been obtained, but the holographic laboratory has been fully equipped at present, and several experiments are in progress.

1. Preparation of Rare-Earth Iron Compounds

Two principal methods seem appropriate for the preparation of the rare-earth-iron compounds: arc-melting of an appropriate mixture of the pure elements, and the addition of the solid rare earth to molten iron in a crucible. Most of the results obtained to date on such properties as magnetostriction in these compounds have utlized specimens prepared by arc melting[2]. As a result, it was decided to attempt the preparation of such compounds as $TbFe_2$ using the second of the two methods listed above, in order to determine the influence of the method of preparation on the magnetic and magnetoelastic properties of interest.

Specimens of terbium-iron compounds have been prepared in this program in the following manner: A crucible containing iron of 99.9% purity was placed in an argon atmosphere and subjected to the rf magnetic field from a 10 kW commercial induction heater. When the iron reached the melting point, the terbium was added to the melt slowly until the correct proportion for $TbFe_2$ was reached. The resulting mixture was then allowed to cool slowly.

Analysis of the specimens by standard metallographic and X-ray techniques is in progress, but no definitive results have yet been obtained. It is anticipated that measurements will soon be made on specimens which have been annealed in a sealed tantalum

crucible for long periods at a temperature near the melting point of the terbium-iron compound.

2. Measurement of Magnetostriction by Holographic Interferometry

The use of holographic interferometry, in which small displacements or deformations of an object can be measured by means of optical interference between the object itself and a holographic three-dimensional image of the object, is a very useful technique in many areas of present-day technology[43]. In the research program described here, the method of holographic interferometry is being employed for the measurement of magnetostriction in rare-earth elements, alloys, and in rare-earth-iron compounds. A two-watt argon-ion laser operating at a wavelength of 514.5 nm is employed for both the recording and the reconstruction of a holographic image of the specimen, which is placed between the poles of an electromagnet capable of producing a field as high as 12 kOe. A real-time method of holographic interferometry is used, in which the photographic plate is exposed and processed in place, without mechanical movement. The hologram is exposed and the image reconstructed with the plate immersed in water, in order to prevent an expansion or contraction of the emulsion between exposure and reconstruction. The processed hologram thus permits the reconstruction of an image which is in exact coincidence with the

original object. If the object is then displaced or deformed due to magnetostriction or other effects, an interference pattern is established between the object and its holographic image. With proper interpretation, the displacement of any point on the object from its position at the time the hologram was formed can be deduced. From the displacement, any component of the strain can be calculated, and, in particular, the presence of inhomogeneous strain can readily be detected. Since the interference pattern is established between the object and an exact image of itself, the shape of the object is relatively unimportant. Thus, small crystals of the type often obtained through strain-annealing can easily be studied.

At present measurements have been made on magnetostriction in commercially prepared specimens of a terbium-iron specimen (the same specimen used to prepare the thin films described in Section III). Typical examples of the interference patterns which are obtained are shown in Fig. 18. In this figure, the interference patterns obtained with two values of the applied field are shown. The terbium-iron specimen is in the form of a cylinder of diameter approximately 0.75 cm and length 1.5 cm, with its axis parallel to the applied field. It should be noted that the applied field for both examples is rather small, in order to display well separated interference fringes. The number of observable fringes at higher

(a) The applied field is 700 Oe.

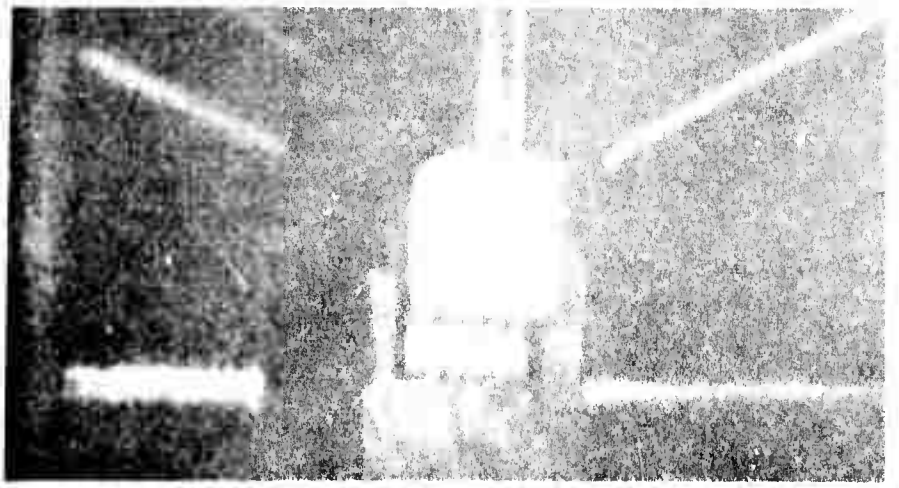

(b) The applied field is 1100 Oe.

Fig. 18. Holographic interferometry, showing the change in interference fringes due to magnetostriction in a polycrystalline terbium-iron cylinder as the applied field is varied.

values of the applied field is so large that magnification is required in order to resolve them.

A preliminary analysis of the magnetostriction of the available specimen of the terbium-iron compound indicates a slightly smaller magnetostriction than that reported by Clark and Belson[2], but this difference does not seem significant, since the demagnetizing factors in the two experiments are undoubtedly different.

A complete analysis of the results obtained with the present specimen is in progress. Further measurements are planned with other iron-rare-earth compounds to be prepared in this program, as described in Section V.1, and measurements are also planned on single-crystal specimens of the pure rare earths and on rare-earth alloys as soon as a cryostat suitable for this work is completed. It is expected that information concerning the rare-earth materials and their magnetostrictive properties can be obtained through the method of holographic interferometry which would be difficult to acquire through more conventional techniques.

REFERENCES

1. P. L. Donoho, F. R. Brotzen, K. Salama, and L. V. Benningfield, Annual Technical Report (2 Nov. 1970-1 Nov. 1971), D.O.D. Contract No. DAAHO1-71-C-0259.
2. A. E. Clark and H. S. Belson, A. I. P. Conf. Proc. 5, 1498 (1972).
3. K. Salama, P. L. Donoho, and F. R. Brotzen, IEEE Ultrasonic Symposium (1971).
4. K. Salama, F. R. Brotzen, and P. L. Donoho, J. Appl. Phys., Aug. 1972 (to be published).
5. A. E. Clark, B. F. deSavage, and R. M. Bozorth, Phys. Rev. 138, A216 (1965).
6. M. P. Maley, P. L. Donoho, and H. A. Blackstead, J. Appl. Phys. 37, 1006 (1966).
7. F. A. Turov and Yu. P. Irkhin, Phys. Metals Res. 3, 15 (1956).
8. C. Kittel, Phys. Rev. 110, 836 (1958).
9. A. I. Akhiezer, V. G. Bariakhtar, and S. V. Peletminskii, Soviet Phys.-JETP 35, 157 (1959).
10. E. Schlömann, J. Appl. Phys. 31, 1647 (1960).
11. M. H. Seavey, Jr., Proc. IEEE 53, 1387 (1965).
12. H. Matthews and R. C. leCraw, Phys. Rev. Letters 8, 397 (1962).
13. B. Lüthi, Appl. Phys. Letters 6, 234 (1965); ibid. 8, 107 (1966).
14. T. J. Moran and B. Lüthi, Phys. Rev. 187, 710 (1969).

15. M. Boiteux, P. Doussineau, B. Ferry, J. Joffrin, and A. Levelut, Phys. Rev. B 4, 3077 (1971).

16. T. J. Moran and B. Lüthi, J. Phys. Chem. Solids 31, 1735 (1970).

17. M. Long, Jr., A. R. Wozzan, and R. Stern, Phys. Rev. 178, 775 (1969).

18. B. R. Cooper, Solid State Phys. 21, 393 (1968).

19. C. S. Barrett and T. B. Massalski, Structure of Metals, New York: McGraw-Hill (1966), p. 631.

20. E. Callen and H. Callen, J. Phys. Chem. Solids 27, 1271 (1966).

21. D. E. Hegland, S. Legvold, and F. H. Spedding, Phys. Rev. 131, 158 (1963).

22. R. J. Pollina and B. Lüthi, Phys. Rev. 177, 841 (1969).

23. C. W. Garland, in Physical Acoustics VII, W. P. Mason and R. N. Thurston, eds., New York: Academic Press (1970).

24. B. Lüthi, T. J. Moran, and R. J. Pollina, J. Phys. Chem. Solids 31, 1741 (1970).

25. K. Tani and H. Mori, Prog. Theor. Phys. 39, 876 (1968).

26. G. E. Laramore and L. P. Kadanoff, Phys. Rev. 187, 619 (1969).

27. K. Kawasaki, Solid State Commun. 6, 57 (1968).

28. L. P. Kadanoff and J. Swift, Phys. Rev. 166, 89 (1968).

29. K. P. Belov, G. I. Kataev, and R. Z. Levitin, Soviet Phys. JETP 10, 670 (1959).

30. L. D. Landau and J. M. Khalatnikov, Dokl. Akad. Nauk SSSR 96, 469 (1954).

31. D. T. Peterson and E. N. Hopkins, Metals, Ceramics and Materials (UC-25) TID-4500 (Oct. 1, 1964).

32. M. Rosen, Phys. Rev. 174, 504 (1968).

33. H. Wagner (unpublished), reported by B. Lüthi et al., J. Phys. Chem. Solids 31, 1741 (1970).

34. L. Holland, Vacuum Deposition of Thin Films, London: Chapman and Hall, Ltd. (1956) p. 21.

35. N. Tsuya, A. E. Clark, and R. M. Bozorth, Proc. Int. Conf. Magnetism, London: Institute of Physics (1965) p. 250.

36. Y. Kikuchi, in Ultrasonic Transducer Materials, O. E. Mattiat, ed., New York: Plenum Press (1971) p. 1.

37. H. Watanabe, Operator Methods in Ligand Field Theory, Englewood Cliffs: Prentice-Hall (1966).

38. L. V. Benningfield, Jr. and P. L. Donoho, J. Physique (France) 32, C-1 233 (1971).

39. H. Bartholin and C. Bloch, J. Physique (France) 32, C-1 235 (1971).

40. H. Goldstein, Classical Mechanics, Reading: Addison-Wesley (1950) Ch. 11.

41. E. Callen and H. B. Callen, Phys. Rev. 139, A 455 (1965).

42. R. Guermeur, J. Joffrin, A. Levelut, and J. Penné, Solid State Comm. 5, 369 (1967).

43. R. J. Collier, C. B. Burckhardt, and L. H. Lin, Optical Holography, New York: Academic Press (1971) Ch. 15.